

**PUBLISHED PROJECT REPORT PPR852**


**Monitoring and Modelling of Landslides in  
Scotland**

Characterisation of Slope Geomorphological Activity and the  
Debris Flow Geohazard

B Sparkes, S A Dunning, M Lim and M G Winter

B Sparkes, Northumbria University.  
 S A Dunning, Newcastle University.  
 M Lim, Northumbria University.  
 M G Winter, TRL Limited.

## Report details

<b>Report prepared for:</b>	Transport Scotland, TRBO		
<b>Project/customer reference:</b>	Transport Scotland Research MFA 2012-010 Monitoring and Modelling		
<b>Copyright:</b>	© TRL Limited		
<b>Report date:</b>	15/03/2018		
<b>Report status/version:</b>	Issue 1		
<b>Quality approval:</b>			
M G Winter (Project Manager)		H Viner (Technical Reviewer)	14/03/2018

## Disclaimer

This report has been produced by TRL Limited (TRL) under a contract with Transport Scotland. Any views expressed in this report are not necessarily those of Transport Scotland.

The information contained herein is the property of TRL Limited and does not necessarily reflect the views or policies of the customer for whom this report was prepared. Whilst every effort has been made to ensure that the matter presented in this report is relevant, accurate and up-to-date, TRL Limited cannot accept any liability for any error or omission, or reliance on part or all of the content in another context.

When purchased in hard copy, this publication is printed on paper that is FSC (Forest Stewardship Council) and TCF (Totally Chlorine Free) registered.

## Contents amendment record

This report has been amended and issued as follows:

Version	Date	Description	Editor	Technical Reviewer
Draft 1b	20/12/2017	Draft	B Sparkes	M G Winter, M Lim, S Dunning
Draft 1f	24/01/2018	Draft	B Sparkes	M G Winter
Draft 1g		TR and Transport Scotland Review	B Sparkes	M G Winter
Draft 1j	01/03/2018	Final edit	B Sparkes	M G Winter
Issue 1	15/03/2018	Published version	M G Winter	H Viner

<b>Document last saved on:</b>	15/03/2018 14:59
<b>Document last saved by:</b>	Reviewer

---

## Table of Contents

Table of Contents	i
List of abbreviations	iii
Executive Summary	2
1 Introduction	4
1.1 Monitoring for greater insight	4
1.2 Modelling the unseen and unknown	6
1.3 Study Sites	6
2 Background	8
2.1 Rest and be Thankful – Past Activity	8
3 Monitoring	10
3.1 Methodology	10
3.2 Results	15
3.3 Discussion	24
4 Modelling	26
4.1 Methodology	26
4.2 Results	30
4.3 Discussion	40
5 Summary and Recommendations	42
6 Conclusions	44
Acknowledgements	46
References	48



---

## List of abbreviations

DEM	Digital Elevation Model
GIS	Geographical Information Systems
LoD	Level of Detection
RAMMS	Rapid Mass Movement Simulation
RabT	Rest and be Thankful
SDLS1	Storm Desmond Landslide 1
SDLS2	Storm Desmond Landslide 2
SFLS1	Storm Frank Landslide 1
TLS	Terrestrial Laser Scanning



---

## Executive Summary

Landslides cause potentially costly damage and disruption to Scottish road infrastructure. Debris-flows, a fast-moving torrent of solids mixed with water, are by far the most frequent cause of such disruption and are capable of causing significant impacts, due to their high mobility. Many debris flow events have been recorded across Scotland, particularly at the highly active A83 Rest and be Thankful (RabT). The influence of gullies in amplifying the hazard from these failures is well understood, and much work has been carried out to characterise the way that rainfall intensity-duration influences slope activity. Until recently, smaller sediment movements and failures have proven difficult to quantify and thus questions have remained over their potential significance. However, small changes on the slope may also have the potential to highlight wider geomorphological controls of activity that are not so well understood. Observations alongside accurate volume estimations may aid the long-term understanding of hazards as well as potentially proving helpful in the consideration and design of management and mitigation measures.

Advances in long range Terrestrial Laser Scanning (TLS) have opened up opportunities to record such changes. This report presents the primary findings of a two-year monitoring project at three sites on the Scottish trunk road network. Seasonal variations in vegetation make comparisons of surveys undertaken at different times of the year difficult. This problem arises from the cyclic growth and decline of widespread bracken cover, which introduces false change signals that obscure real geomorphic changes. A tailored monitoring workflow has been developed for sites that undergo such significant seasonal vegetation changes, enabling the detection of slope material losses smaller than 1 m<sup>3</sup>. Monitoring has been carried out at two to three month intervals at the A83 RabT, and a slightly lower frequency at the A82 Glen Coe and A85 Glen Ogle.

In total, six shallow failures have been detected and, where possible, quantified at RabT during the monitoring period. A number of secondary mobilisations and other changes have also been detected; these other changes potentially represent long-term precursors and should be re-analysed in the context of future events. A limited number of changes have been detected at the A82 Glen Coe and A85 Glen Ogle sites, although a large rockfall was detected some distance from the A82 carriageway prompting an inspection by the road authority.

A key finding of the monitoring has been the segregation of slope failure processes into either the modification of existing hillslope gully systems (producing net deposition or scour), or the development of new channels (< 0.5m depth) or gullies (≥ 0.5m depth). Both effects are significant, as they may result in the release of otherwise relatively immobile sediment stores. Sub-annual monitoring at RModelling of difficult to observe abT (monthly where weather permits) has further highlighted secondary mobilisations from landslide scars, up to one year after failure. For instance, a 224 m<sup>3</sup> secondary mobilisation, days after the initial failure associated with Storm Desmond (labelled SDLS2 – Storm Desmond Landslide 2), may have reduced the retention capacity of a debris flow catch net. The same net was later subject to a flow associated with the Storm Frank (SFLS1 – Storm Frank Landslide 1) flow, from which material reached the A83 carriageway. Quantification of the SDLS2 event, particularly the loss of 85 % of the failed mass to a nearby gully, has also demonstrated the potential for smaller events to recharge gullies with significant quantities of sediment for

later entrainment. This process has previously resulted in debris flow hazard amplification; the largest recorded debris flow recorded at RabT (October 2014) almost doubled in magnitude as a result of entrainment, resulting in closure of the A83.

To further develop the hazard assessment of the most active of the monitored sites, the A83 RabT, two modelling approaches are presented; these are numerical modelling of debris flow propagation and simulation of likely hydrological flow lines over the slope. Back-analysis and calibration of the former has been found to yield realistic deposition distributions, demonstrating the credibility of the model to simulate events at A83 RabT and thus perform hazard-analysis. The initial experimental hazard modelling results suggest that such an approach could be very powerful, enabling both zones of relatively high mobility and potential gaps in current mitigation efforts to be identified. This approach does however require further development, with particular focus required around whole-slope coverage and increased resolution to account for sources on inter-channel ridges; these may be split and flow into multiple channels and do not give a true indication of mobility potential.

Modelling of difficult to observe hydrological pathways shows some promise in demonstrating the potential role of water flow in triggering some shallow failures. Model results appear to corroborate on-slope evidence of small ephemeral drainage channels, which may be of significance to shallow failure initiation and gully development. A larger collection of TLS derived change may be required to fully substantiate this theory. Continued TLS monitoring would be beneficial for this purpose and has already proven beneficial through the identification of at least six additional small failures at A83 RabT following the original two-year monitoring period, the results of which are presented in this report.

Multiple surveys around the winter months are advised for RabT, whilst annual change might be of benefit at A82 Glen Coe. Lower frequency surveys, every few years, may be appropriate for the A85 Glen Ogle site in order to assess steady-state sediment dynamics.



# 1 Introduction

Landslides cause major disruption and socio-economic damage around the world. This is particularly the case in developing countries, where anticipation and mitigation of landslide hazards may be lacking. Whilst landslide hazards are better managed in developed countries, their capacity to disrupt communities and incur appreciable economic costs remains evident. Debris flows are a particularly mobile type of landslide owing to a large constituent quantity of water amongst mud and coarse debris. Debris flows in the west of Scotland are typically triggered by intense rainfall and thus often coincide with some of the wettest months, namely those falling between September and January (Winter et al. 2010). Recent climate change forecasts anticipate an increased incidence of intense rainfall events in the UK, and thus potentially an upturn in debris flow activity (Winter & Shearer 2014), which could in turn pose a continued or greater hazard to road infrastructure.

Knowledge of potential debris flow sources, magnitude and runout are crucial to effective hazard assessments (Iverson 2014). Events at sites across Scotland have been well documented, from relatively early mapping and lichenometric dating by Innes (1983), to subsequent publications by, for example, Ballantyne (1986), Winter et al. (2005; 2006; 2009), Milne et al. (2009), the British Geological Survey (BGS 2007) and Strachan (2015), not to mention several unpublished geotechnical reports. Many reports focus on events that have impacted infrastructure, often roads, in some way and do not generally incorporate smaller changes as these can remain undetected. These smaller events, including those that do not reach infrastructure, can offer valuable insight into processes that are important indicators of future larger changes.

Channel confined events represent a more significant hazard than hillslope events, as momentum is sustained and large quantities of further material and water can be entrained; entrainment of saturated sediments has been shown to increase debris flow mobility (Iverson et al. 2011). Because channels represent a source of hazard amplification, it is possible to focus mitigation efforts such areas of a slope. Each channel (< 5m depth) or gully ( $\geq 0.5$ m depth) (Bocco, 1991) represents a unique hazard. Variations in factors such as size, material depth and properties, sinuosity, undulation and slope angle invariably influence the potential for hazard runout. Variations in sediment accumulations between gullies may also be significant.

This report presents research undertaken as part of a doctoral project at Northumbria University partnering with the Transport Research Laboratory (TRL) and funded by the Scottish Road Research Board (SRRB), Transport Scotland and Northumbria University. The research has focused on the remote monitoring of several landslide prone sites in Scotland, with a particular focus on the A83 Rest and be Thankful (RabT), where numerical runout modelling has also been applied, with monitoring also carried out at the A82 Glen Coe and A85 Glen Ogle.

## 1.1 Monitoring for greater insight

Landslide processes have historically been difficult to observe in detail, a problem exacerbated by their destructive nature and the inaccessibility of many sites (Iverson 1997). Much progress has been made in the field of debris flow science, particularly through

observations and records of the phenomena from the 1960s (Takahashi 2014) and greater understanding of the ability for rocks and debris to flow like a fluid (Davies 1982). Many early advances in the field stemmed from the use of experiments and models, although these were often highly idealised (Iverson 1997).

Questions relating to debris flows, such as their initiation, interaction with other geomorphological processes, and activity in a changing climate, still remain however. Our understanding of runoff initiated debris flows is for instance relatively lacking (Kean et al. 2013), particularly where small juvenile or transient channels occur. Investigations of hillslope failure scar development is also particularly lacking (Johnson and Warburton 2015). With greater deployment of structures such as catch nets, pits and large engineered culverts, it becomes vital to characterise shallow landsliding, debris flow behaviour, sediment dynamics and slope development.

Statistical analysis of landslide magnitude and frequency is useful in assessing rates of hazard recurrence at a site. It is also important to assess the potential for magnitude increase through entrainment of gully sediment stores which can directly influence geohazard potential (Milne et al. 2010). An understanding of the largest credible, or other, hazard at a site can be used to inform the design of mitigation structures (Bovis & Jakob 1999), ensuring that such efforts are appropriate and reduce landslide risk to the desired extent (Winter 2014). Under-informed design can result in inefficient mitigation; flow events can exceed design capacities, resulting in road closures. Furthermore, it is not yet understood whether efforts should be focused on areas of past activity or slope areas in which change or other geomorphic activity is evident. Through monitoring, perhaps over several years, the latter could prove important as a precursor to eventual slope failure. It may also be possible to develop a more efficient approach to mitigation, as some slope areas could prove relatively inactive, due to exhausted sediment stores for example.

Large magnitude landslides rarely go undetected, however smaller failures are hard to detect and are often under-reported, particularly when such events do not affect infrastructure. This problem relates, in-part, to difficulties observing the smallest magnitude failures and changes, as well as differentiating between these and other features or relict scars. This can easily skew our understanding of the phenomenon, particularly their magnitude and frequency.

Recent advances in remote sensing are now capable of objectively highlighting small changes slope wide, changes which may have previously remained unrecorded (Lim et al. 2005; Rosser et al. 2007), even at ranges of several kilometres (Fey & Wichmann 2017). Such activity may yield insight into an important and more holistic geomorphological understanding (Neugirg et al. 2016). Repeat Terrestrial Laser Scanning (TLS) is a particularly useful form of monitoring which has resulted in major findings relating to debris flows, as well as other geophysical phenomena. Schurch et al. (2011) have for example shown that debris flow depth exerts a fundamental control on the rates of channel erosion.

TLS-based monitoring is a major improvement over previous single-point measurement approaches, as landslide kinematics and failure mechanisms can be examined in far greater detail (Jaboyedoff et al. 2012). Accessing hillslopes, particularly initiation zones demonstrating a high frequency of observable activity, has however proven a significant challenge, hindering holistic monitoring attempts. Frequent activity in Scotland, at

accessible sites with relatively limited relief, affords the opportunity for more holistic observations, from ‘source to sink’.

## 1.2 Modelling the unseen and unknown

Whilst monitoring may aid our understanding of the spatial distribution of slope activity high up on the slope, conventional magnitude and frequency analysis alone does not account for variability in hazard at road level, towards the foot of the slope. This necessitates the combination of such knowledge with susceptibility analysis (Corominas & Moya 2008). Empirical-statistical models have accounted for several individual influences on flow propagation, such as deceleration at channel bends (Benda & Cundy 1990). However dynamic (numerical) models consider momentum conservation in a more holistic sense (Rickenmann 2005). These models are effective at assessing the influence of topography on flow, achieved through input of a digital elevation model (DEM) and numerical simulation of idealised flow cells over the model.

Debris flow models have progressed significantly over the last decade (Delannay et al. 2017), with recent developments in their GUIs (Graphical User Interface) arguably improving the ease with which propagation can be predicted. Models can be used to produce hazard maps of both extent and severity (Petrascheck & Kienholz 2003). Furthermore, even with advances in long-range remote monitoring techniques, gathering of complete observation data remains a difficult task. Idealised models have previously been used to improve the understanding of debris flow mechanics (Iverson 1997) and may prove useful in supplementing TLS data where occlusion or data gaps have occurred. Data in oblique and wet areas, typical of channels with steep banks, is often lacking for example, however these areas are where debris flow deposition or erosion are most likely to occur.

High resolution survey data, such as that collected through TLS as part of this study, is of great value to numerical modelling (Dietrich & Krautblatter 2017) and offers many benefits over lower-resolution alternatives. Aerial photographs alone, whilst offering an accurate depiction of a landslide domain, do not provide an accurate impression of the source depth and thus the true magnitude of the landslide. TLS data has been used to back-analyse a numerical runout model as part of this project, in order to overcome sources of magnitude uncertainty and to aid further analysis and assessment. These data have also aided the mapping of slope hydrology, in order to better interpret and understand the findings from the two-year monitoring study.

## 1.3 Study Sites

Three study sites (Figure 1) have been repeatedly surveyed over the course of the two-year monitoring study. These sites include the A83 RabT, A85 Glen Ogle and A82 Glen Coe. RabT has been particularly active as discussed later in this report. The A85 Glen Ogle site is particularly well known for a series of debris flows in 2004 which resulted in helicopter evacuations of road users trapped between two of the flows (Winter et al. 2005; 2006; 2009). Whilst Glen Ogle has demonstrated limited slope activity since 2004, stratigraphic evidence suggests multiple instances of historic landsliding (Milne et al. 2009) and thus potential for further future activity. Both A83 RabT and A85 Glen Ogle are characterised by

schistose bedrocks topped by a more susceptible layer of colluvium and soil. The RabT has a particularly high gully count, much higher than that of A85 Glen Ogle; gullies are considered to potentially play a major role in the frequency of hazard activity at sites such as RabT.

In contrast to RabT and Glen Ogle, the A82 at Glen Coe has experienced limited disruption by landsliding since events that occurred in the late-1980s/early-1990s. The site is characterised by much steeper bedrock faces with a number of incised gullies, whilst sediments are limited to much coarser debris at the foot of the steep rock faces. Gullies throughout the Pass of Glencoe may however also contain accumulations of degraded sediment. The pass is particularly popular with tourists and popular rest stops for viewing the outstanding scenery and reaching trail heads are situated proximal to the slopes, raising concerns about the potential effects of geohazards at the site.

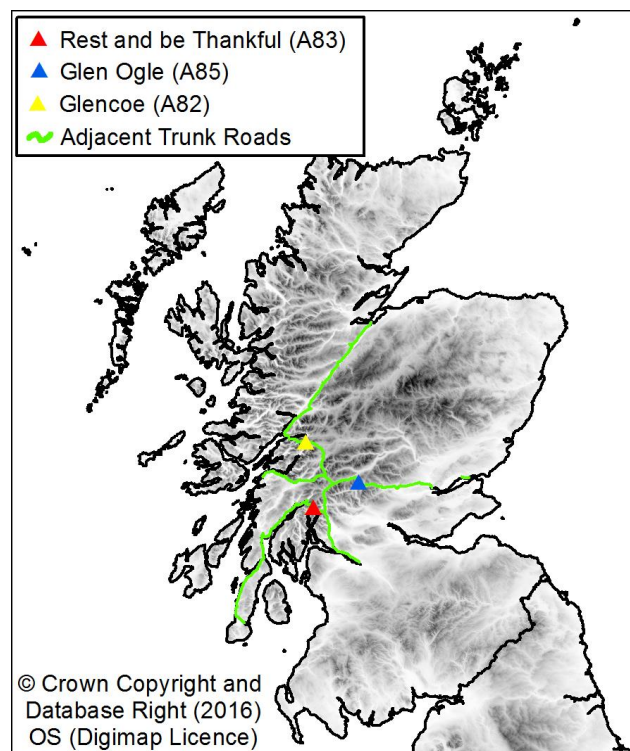


**Figure 1. A map of the study sites monitored throughout a two-year research project.**

## 2 Background

Scottish transport infrastructure, particularly roads, has been impacted by a number of landslide events in recent years. Active sites within the last 15 years include, among others, the A9 at Dunkeld, the A83 RabT, A83 Cairndow, A85 Glen Ogle, A887 Invermoriston and A83 Glen Kinglas (Winter et al. 2005; 2006; 2009). The A83 RabT has been particularly active, with more than 20 failures recorded at the site since 2004. This high frequency of activity, as well as the accessibility of the site, makes it ideal for the investigation of debris flow processes and the nature of the geohazard.

### 2.1 Rest and be Thankful – Past Activity

The RabT has become well-known for its high frequency of slope activity and the associated disruption to the A83 trunk road and to the communities it serves. The region is one of the wettest in the UK (> 3,000 mm/yr; Met Office 2016), with rainfall the key trigger for failure. The rate of activity at RabT is however far from unprecedented in Scotland, especially when accounting for variations in mean annual rainfall across the country (Sparkes et al. 2017) and potentially high rates of unrecorded activity elsewhere.

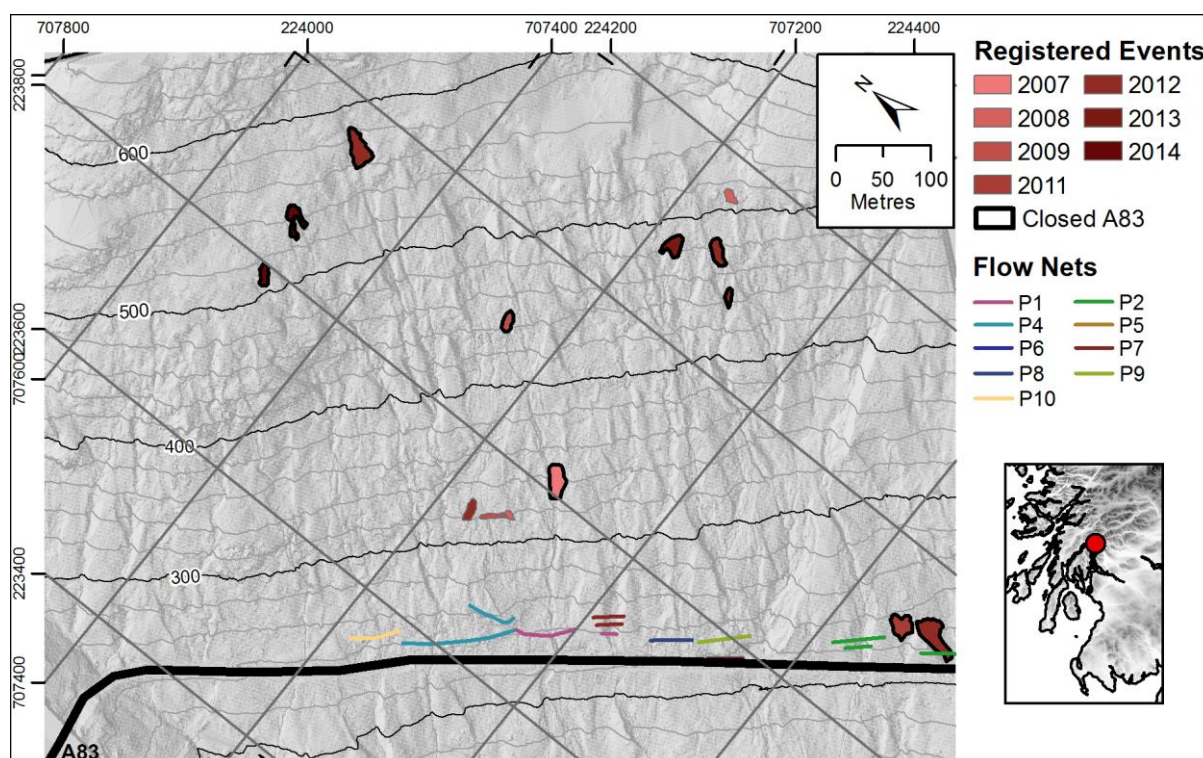


**Figure 2. A spatial inventory of events at A83 RabT up to 2014.**

A series of reports was synthesised and collated to produce a spatial inventory of events at RabT (Figure 2) that occurred prior to the start of the monitoring presented herein. A large proportion of slope failures has resulted in road closures. More recently, mitigation efforts, such as debris flow catch nets, have diminished the impact of similar failures. The first phase 1 net was installed in 2010, after which subsequent catch nets were installed until 2013, since which further works have been carried out. Debris flows are still capable of disrupting

---

the road and inflicting costly damage – large magnitude events such as that recorded in October 2014 (> 1,000 tonnes) are particularly problematic and thus a greater understanding of the causes and mechanisms of such events is vital. Detection of small changes or other activity could signal a precursor to a large magnitude event, either in the short-term (< 12 months) or over a much longer-term (many years). Such an event may grow through mobilisation and entrainment of sediment stores, which monitoring may be capable of highlighting. RabT was chosen as an ideal site for high frequency surveys (monthly to quarterly).

### 3 Monitoring

Terrestrial Laser Scanning (TLS) surveys have been conducted at three sites over a two-year period. In addition to RabT (A83), both Glen Ogle (A85) and Glen Coe (A82) have experienced mass slope movement in the past. Glen Ogle experienced the most significant activity in 2004 when two large debris flows, among others, propagated from the slope and blocked the A85 trunk road (Winter et al. 2006). Questions have been raised about potential ongoing activity at both sites and whether these could be detected and be signal precursors to future events. These sites have therefore also been chosen for monitoring alongside RabT, Monitoring was at a lower frequency (quarterly) as there had been relatively little reported activity in recent years. Table 1 shows the survey programme carried out at all three sites.

**Table 1 – The survey programme at all three study sites.**

	2015												2016												2017			
	1	2	3	4	5	6	7	8	9	10	11	12	1	2	3	4	5	6	7	8	9	10	11	12	1	2	3	4
RabT			1	3			5		8	10		13		14		16	19		21		22		25	27	29	30	31	
Glen Ogle			2	4			6		9	11					17	20					23		26				32	
Glencoce							7			12				15	18						24			28			33	

#### 3.1 Methodology

A long-range laser scanner, the Riegl LMS-Z620 (2 km range), has primarily been used to collect topographic data for each study site. A Riegl VZ-4000 was also used on two occasions, in July 2016 and April 2017. Data are collected in point cloud format, representing X, Y and Z cartesian co-ordinates relative to the scanner ( $X = 0$ ,  $Y = 0$ ,  $Z = 0$ ). Several scan positions are used at each study site to ensure total slope coverage and to minimise occlusions. Surveys at RabT were conducted from three scan positions, with two peripheral positions subsequently aligned and registered to a central plinth position. Glen Ogle followed a similar survey set-up, although with four scan positions, whilst Glen Coe contained three sub-sites, each of which necessitated individual scans. The survey set-ups for all three sites are shown in Figure 3.

Data were coarsely aligned within the software package RiScan using four well distributed control points, after which an iterative closest point (ICP) algorithm (Besl & McKay 1992) was applied to tightly match the scans together. Subsections containing minimal vegetation (i.e. rock faces) were used in this latter process to avoid irregularities related to variable laser penetration from different scan positions. The same registration process was used to register each overall scan (multiple stations registered and merged) back to the first co-registered and merged scan dataset (April 2015). Registration has been confirmed using 2D cross-sections within the software package Quick Terrain Modeler. The cumulative uncertainty arising from registrations at RabT was around 0.09 m. Data have been cleaned of perennial vegetation using a mask (first created manually). Co-registered data were further subsampled to a minimum 0.2 m spacing, to produce a relatively evenly spaced point cloud despite an increased range and original point spacing at the top of the slope.

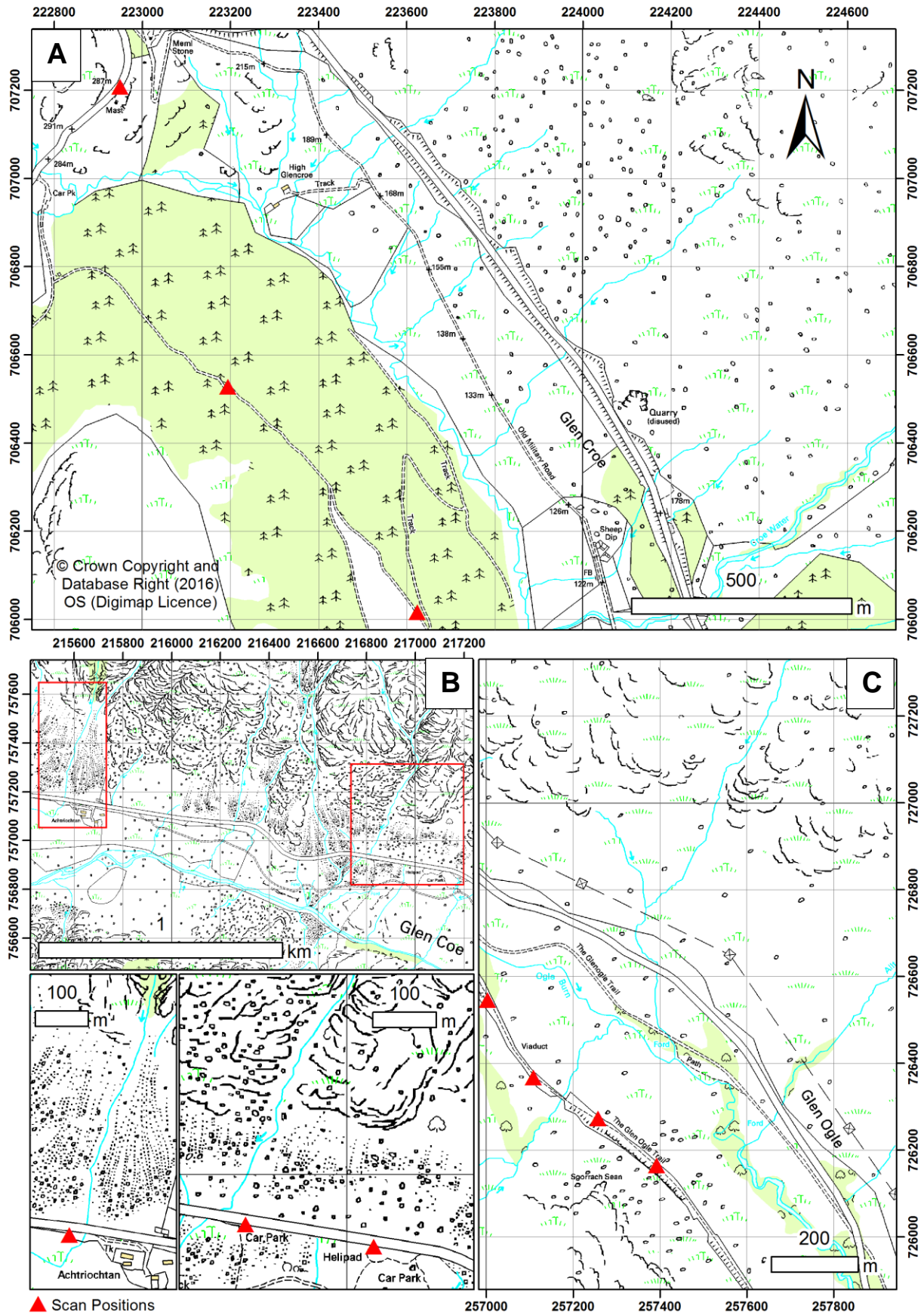
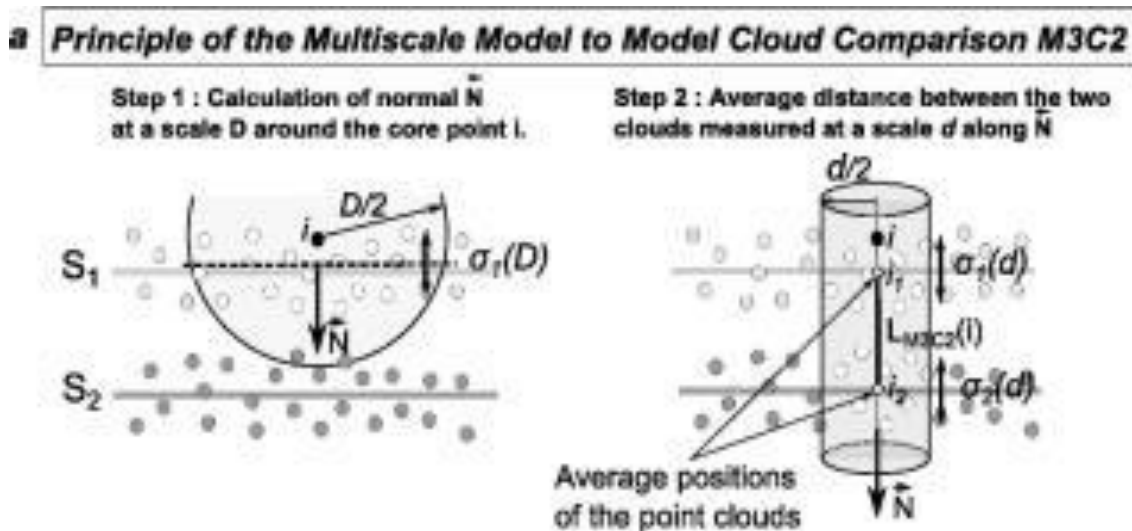


Figure 3 – Survey set-ups at all three study sites.

A) A83 Rest and be Thankful B) A82 Glen Coe (inset boxes below) C) A85 Glen Ogle



Change detection was carried out using the M3C2 algorithm (Lague et al. 2013) implemented within the software CloudCompare. A schematic of this change detection approach is shown in Figure 4. This was applied at an inter-annual scale (i.e. April 2015 to April 2016) as well as an intra-annual scale (i.e. April to May). A workflow was developed for intra-annual change detection, to overcome the impacts of seasonal-vegetation growth and die-back (demonstrated in Figure 5) which is in the same order of magnitude as the shallow landslides to be detected. Sequential scans were compared with a base dataset (i.e. April after winter vegetation dieback).



**Figure 4. A schematic of the M3C2 change detection technique (Lague et al. 2013). Unlike many other simple change detection approaches, M3C2 can appropriately orientate such calculations, negate interpolation related artefacts and account for both point cloud noise and occlusion.**

An uncertainty value (Level of Detection; LoD) of 0.2 m was used to account for both instrument precision and registration error (RMSE), whilst a 1 m cylinder diameter (change domain used by the algorithm) was used for each change calculation and normal (orientation) calculation. Resultant change was filtered for statistical significance (95 % confidence interval), after which outliers (i.e. standalone points) were removed using a density filter.

The remaining change data were migrated to the Geographical Information Systems (GIS) software package ArcMap, a powerful processing environment in which multiple geographical datasets can be plotted, processed and analysed. ArcMap was immediately used to calculate volumetric change information, by multiplying the change domain (3D surface area) by the mean depth of change.

Calculated volumes may underestimate or overestimate the true magnitude of change resulting from compounded instrument and registration errors. Uncertainty related to the depth of change at RabT is  $\pm 0.088$  m, thus an idealised change measuring  $1 \text{ m}^2$ , with 1 m depth, would yield an uncertainty of  $1 \text{ m}^3 \pm 0.088 \text{ m}^3$  (8.8 %). Failures with a mean depth larger than 1 m have a lower relative volume uncertainty, whereas shallower failures have a larger relative volume uncertainty. Furthermore, thresholding of changes below a 0.2 m LoD

may result in omission of changes and thus a further underestimation of the true change magnitude, one of the shortcomings of long-range TLS.

Resultant intra-annual change datasets were processed to remove change prior to the respective dataset. For example, April to May losses would be subtracted from April to June losses, leaving just losses occurring between May and June. This workflow is illustrated in Figure 6 (C).

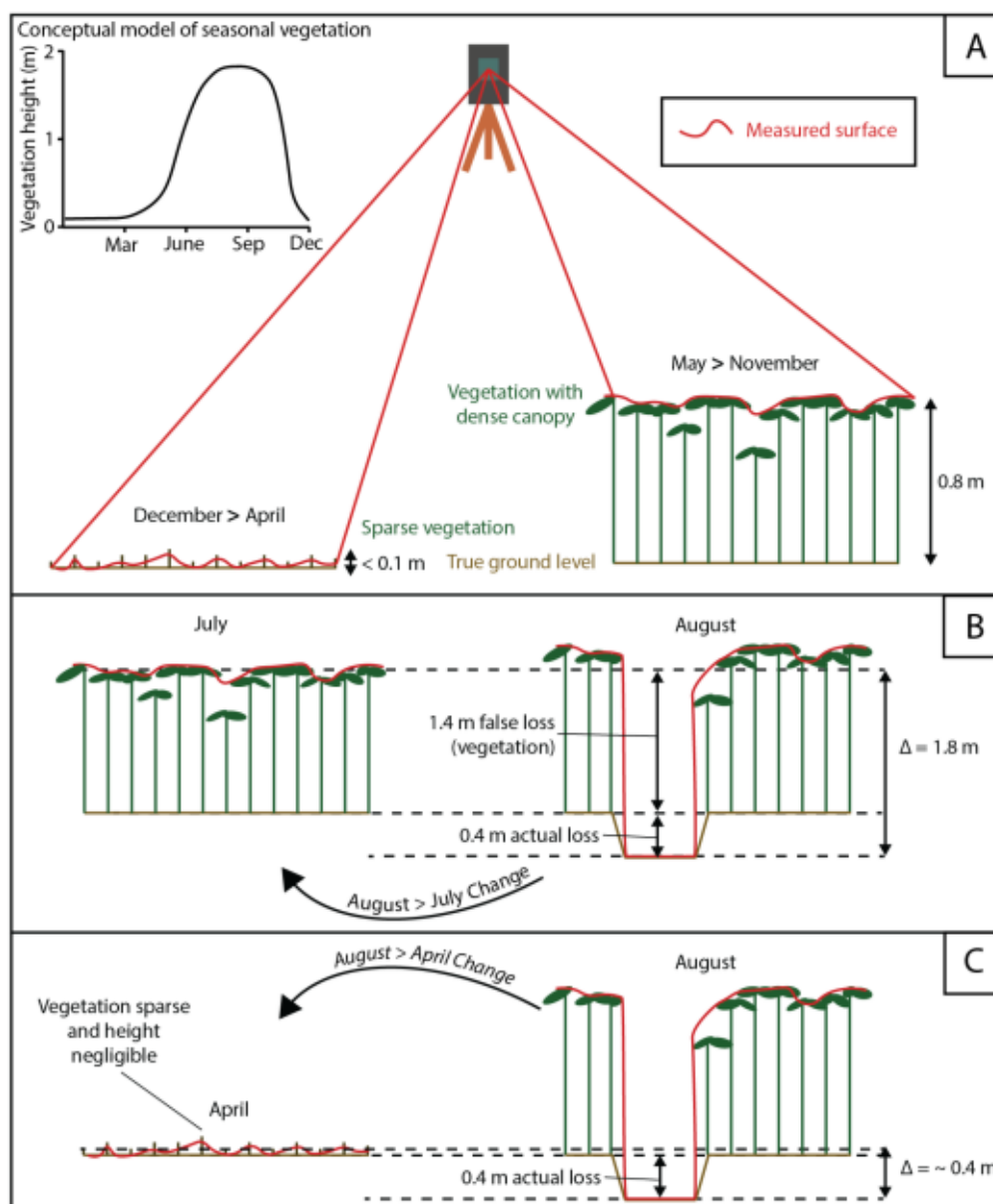


**Figure 5. (A) Problems arise during intra-annual change detection, as vegetation fluxes throughout the seasons (B) This results in an overestimation of ‘true’ loss should vegetation vacate a source as well (C) Comparison with a base dataset enables isolation of ‘true’ loss when ‘gain’ is ignored.**

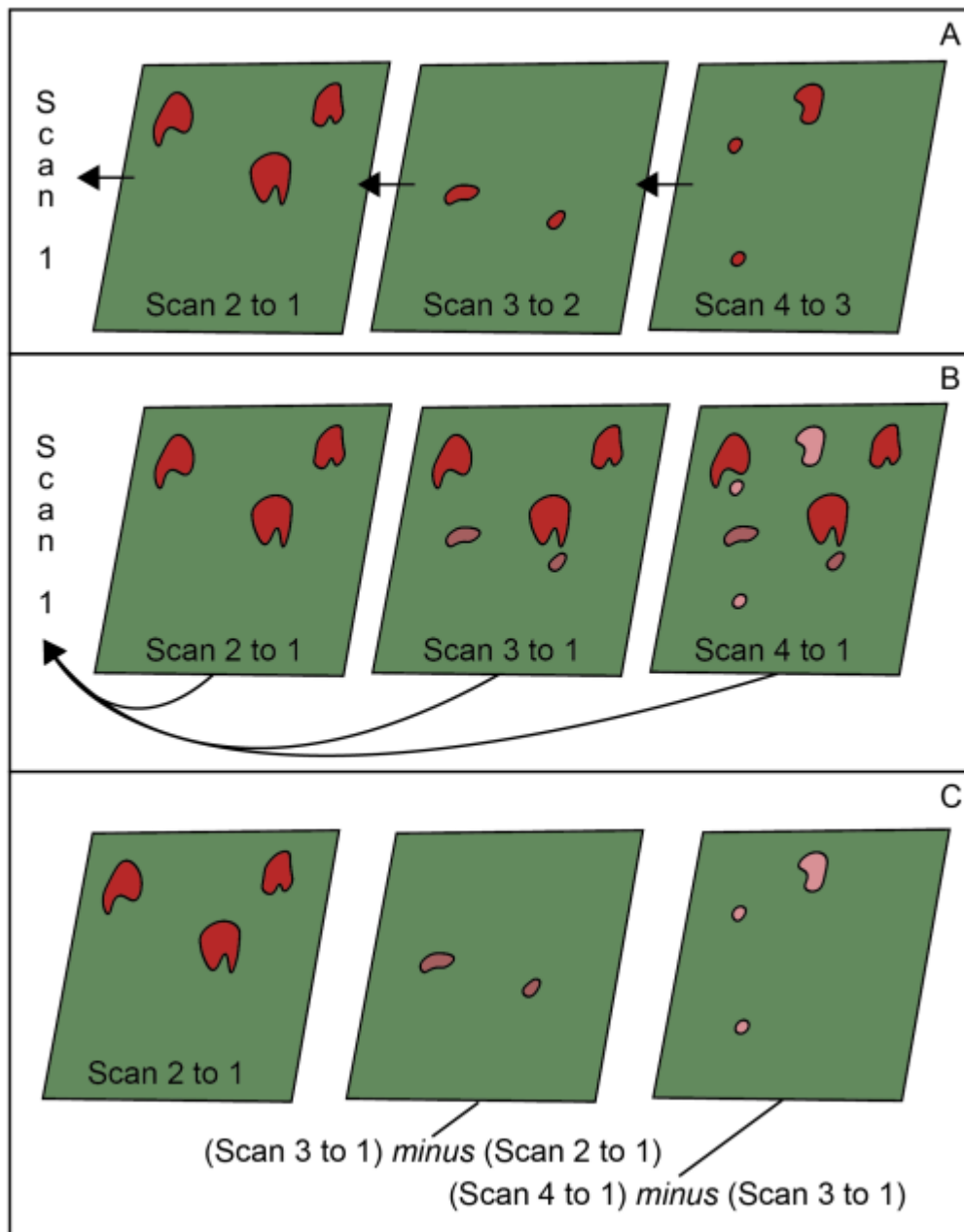


**Figure 6. (A) A conventional change detection approach (B) An unconventional change approach which results in an accumulation of changes from different surveys (C) Masking of preceding change results in isolated change, much like conventional change data. (Sparkes, PhD Thesis in prep).**

---

## 3.2 Results

### 3.2.1 *Rest and be Thankful – Inter-annual change*

Multiple changes occurred at RabT over the two-year monitoring period, most notably the events of December 2015 resulting from storms Desmond and Frank. The main landslides triggered by these storms have been named using the convention SDLS1, SDLS2 and SFLS1 (i.e. Storm Desmond Landslide 1, Storm Desmond Landslide 2 or Storm Frank Landslide 1) and are labelled within Figure 7, among other detected changes. The dates of these events are well constrained due to their notable effects and disruption, particularly those following SFLS1. Other events can only be located within the survey period using the current TLS methods, although this has since proven useful for guidance of supplementary high-frequency photography, generally enabling the isolation of events to a sub-24 hour period.

On 5th December, a shallow failure was triggered by intense rainfall during Storm Desmond (90 mm in 20 hours, up to 8.8 mm/hr), just 80 m upslope of the A83. The failure propagated into a catch net just 20 m above the carriageway. The SDLS1 source area is represented by one single polygon (Figure 7) owing to its large depth (mean 1.5 m, maximum 3 m). The event source was calculated to be 630 m<sup>3</sup> (using the April 2015 to April 2016 datasets). The event also immediately eroded 37.5 m<sup>3</sup> of material from a previously consolidated slope region, leaving a new truncated channel.

Following SDLS1, a higher elevation shallow failure was triggered (SDLS2) on 6<sup>th</sup> December, during Storm Desmond. A source volume of 334 m<sup>3</sup> was calculated using the April 2015 to April 2016 datasets. The majority (85 %) of the source mass propagated into a nearby channel, little of this material (~8 %), inferred from TLS measurements of the deposit height, was found to have accumulated behind two stacked phase 7 catch nets. Laser attenuation (weak signal return) resulted in a lack of data coverage in dark and wet areas of the slope. Gullies were particularly prone to this problem and so precise quantification of deposition in these areas was not possible. It is therefore assumed that approximately 300 m<sup>3</sup> of material was deposited within the gully to the south of the SDLS2 source, although the distribution of this material is not known. The SDLS2 source area was found to be heavily saturated, with concentrated drainage also evident within close proximity, both above and alongside the landslide scar.

On 30th December, during Storm Frank, a third major landslide was triggered by intense rainfall (60 mm rainfall in 12 hours, up to 9.2 mm/hr). The shallow failure initiated from a higher elevation than SDLS2, before eventually propagating into a major gully along which previous failures (2007 and 2009; Figure 2) have been recorded prior to monitoring. Each recorded event appears to have significantly developed the channel. The debris flow propagated to the bottom of the slope where it impacted a phase 1 catch net, the same net that had previously been emptied after arresting SDLS1. On this occasion, the catch net did not retain all of the SFLS1 flow; material from SFLS1 spilled onto the carriageway resulting in a temporary road closure.

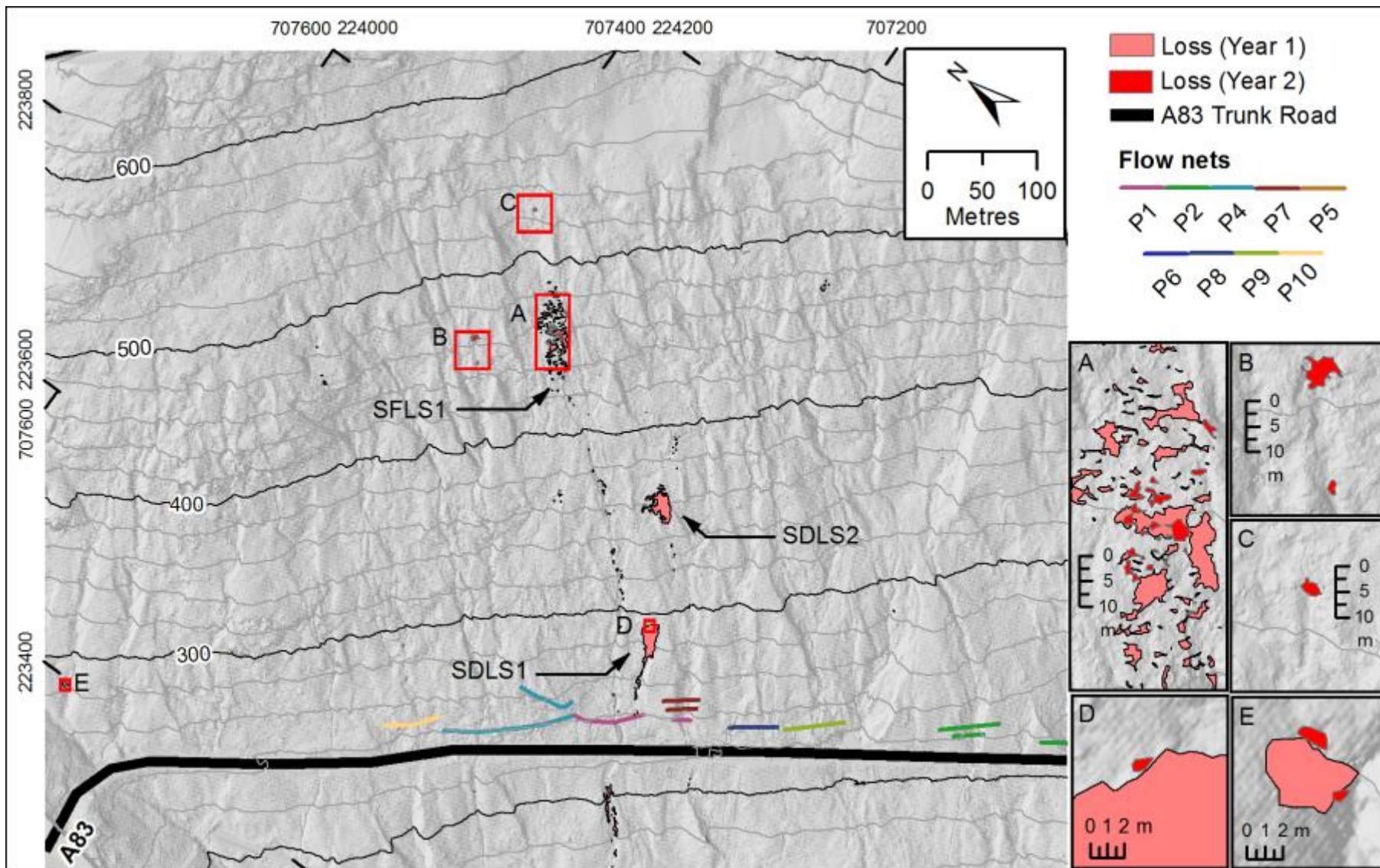


Figure 7. A composite of losses detected in both years 1 and 2 of monitoring.

This disruption was further compounded when an unstable 150 tonne boulder was found within the source area, requiring mitigation work and a road closure. It is not fully understood why material propagated onto the road. However, the marginally larger source area of SFLS1 and the greater opportunity for entrainment and dilution by streamflow are likely explanations. Entrainment was not quantifiable due to gully occlusion and laser-attenuation of the Z620 instrument, however small change polygons indicate at least a small degree of erosion and entrainment within the gully.

A small shallow failure at the margin of a major gully was detected towards the north-east extent of the study area (Figure 7E) prior to the storm events, between 20th April and 29th July 2015. No deposits were detected; the event has fully evacuated its source and moved downstream.

The temporal distribution of the second-year changes is not precisely defined by TLS monitoring, owing to their small size and lack of impact at road level. Many of these second-year changes relate to previous failures and thus demonstrate the 'activating' effect (scour confined within the scar, or retrogression) that large events can have in releasing sediment, even many months after initial failure. Secondary mobilisations include 32.5 m<sup>3</sup> from the source area of SFLS1 (Figure 7A), retreat along the margin of the small landslide source area detected in July 2015 (Figure 7E) and a small loss at the headscarp of SDLS1 (Figure 7D).

Two small shallow failures were also detected high up on the slope (Figure 7B and 7C), again within a central zone. These were estimated to measure 26 m<sup>3</sup> and 8 m<sup>3</sup> respectively, similar in magnitude to the landslide detected in July 2015. Detection of these failures at a high elevation, where survey data is inherently of a reduced point spacing (due to increased laser beam divergence at range), demonstrates the capability of long range TLS monitoring to detect small failures that would have previously been hard to detect.

As well as their position within the centre of the slope, the source areas of these two failures are found to lie along small ephemeral flow lines (visible in this case using the high-resolution photo-mosaics shown in Figure 8 and Figure 9).

#### *3.2.1.1 Post two-year monitoring changes*

Whilst change has not been presented beyond the two-year monitoring period, a further small mobilisation has recently (November 2017) been observed directly above SDLS2, as visible in Figure 10. This small failure is of interest, as it may correspond with and share the same drainage feature observed proximal to the SDLS2 scar. The change is contained within this recently collected TLS data alongside several other changes which will be subject to further analysis at a later date. These data should prove useful in analysing change related to modelled drainage. Furthermore, they may be useful as a source of uninhibited flows for the purposes of runout modelling back-analysis.

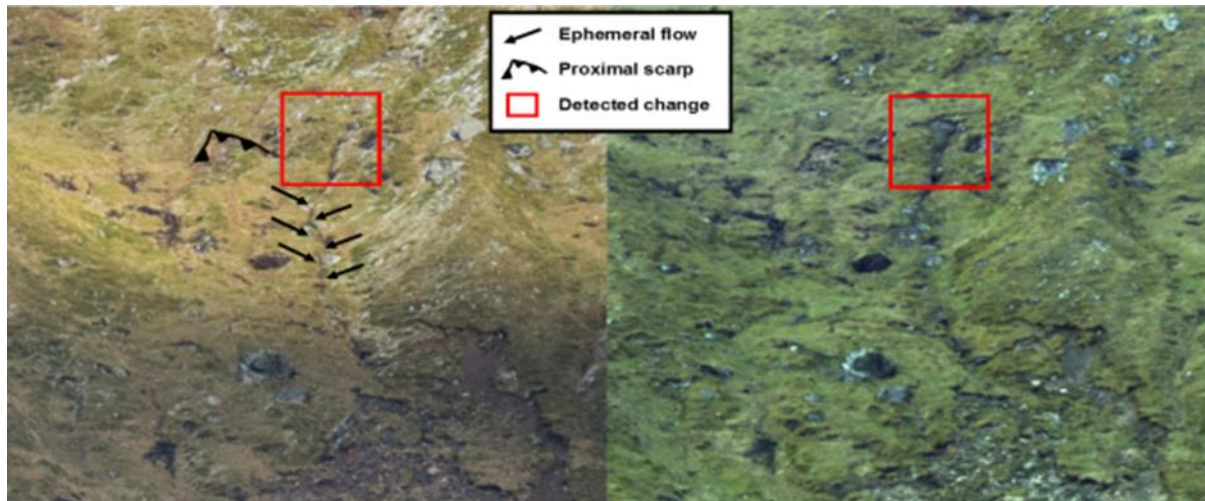


**Figure 8. Photographs taken before and after initiation of the higher elevation small failure (sub-box C in Figure 7). In this, a small incised channel is evident prior to failure.**

**Incidentally this failure occurred directly above the source area of the SFLS1 event, continuing a pattern of failures along the same longitudinal extent. (Sparkes, PhD thesis in prep).**



**Figure 9. Photographs taken before and after another small failure detected in the second year of monitoring (sub-box B in Figure 7). In this case, a truncated tributary channel leading into a more major gully system was evident directly below the source prior to failure. This area of slope also appears to have been saturated prior to failure. A small tension crack has subsequently appeared above the source.**



**Figure 10. A new mobilisation observed directly above SDLS2 (the source demarcated by a red box, in which a monitoring station can just about be observed). This was found beyond the two-year monitoring period, in November 2017.**

### **3.2.2**      *Rest and be Thankful - Intra-annual change*

In this section, the annual change presented in Figure 7 has been masked and changes isolated to their respective survey periods, enabling greater analysis such as more precise timing of the small landslides in the second monitoring year. Intra-annual data has been presented separately to that of the inter-annual data, principally to highlight the merits of each respective technique.

#### **3.2.2.1**      *Year 1*

For the purposes of brevity and aiding interpretation, sequential changes isolated in the first year of monitoring have all been shown in Figure 11. In the first half of the monitoring year (April 2015 to October 2015), the only major changes detected were those of the small July 2015 landslide (A in Figure 11) and reworking of sediments below the carriageway and a



large engineered culvert (D in Figure 11). The latter is mostly obscured in Figure 11 by subsequent changes. However a small amount of loss can be seen to have occurred between September and October 2015.

The second half of the monitoring year was far more active, particularly in December 2015 as previously discussed. Between October and December 2015, the two large landslides SDLS1 and SDLS2 can be seen (Figure 11B and 11C respectively). Much of the SDLS1 source area is obscured by subsequent loss in the next survey period, between December 2015 and February 2016. Whilst a loss of 630 m<sup>3</sup> was calculated during the annual change detection, the intra-annual change shows that the SDLS1 source area experienced at least two discrete mobilisations. The first of these occurred on 5th December and measured 406 m<sup>3</sup>, whilst the second occurred at some time between this date and 11th February (subsequent survey period; December 2015 to February 2016) and measured 224 m<sup>3</sup>. The magnitude of the first mobilisation is more in-line with those discussed by Geobruigg (2015) the manufacturers of the catch net. In the same period as the second SDLS1 mobilisation, a further 12.5 m<sup>3</sup> loss was scoured from within the truncated channel below the source. The emergence of SFLS1 can be seen in the same period (Figure 11E).

During the survey period December 2015 to February 2016, a large quantity of loss (199 m<sup>3</sup>) was detected within the gully below the carriageway and large engineered culvert (Figure 11D). The overall quantity of evacuated material was approximately 140 m<sup>3</sup> (measured within CloudCompare using a simple 2.5D volume tool) when accounting for deposition. During the final survey period (February 2016 to April 2016), further change was detected at the headscarp of the SDLS1 source area (Figure 11b). Losses were also detected at the margins of the earlier July 2015 landslide (Figure 11a). These changes again demonstrate the ‘activating’ effect of initial failures.

#### 3.2.2.2 Year 2

Sequential changes isolated in the second year of monitoring are collectively shown in Figure 12. The smaller degree of change here is evident. The first survey period covers most of the year (April 2016 to December 2016) due to minimal detectable change. This first period is followed by two shorter survey periods covering the winter months (December 2016 to February 2017; February 2017 to April 2017). Changes in the first survey period include small changes related to the SFLS1 and SDLS1 source areas (Figure 12D and 12E respectively), again demonstrating prolonged activity long after initial failure. A small shallow failure, discussed earlier (Section 3.2.1, Figure 7B), was detected in the second survey period (Figure 12B) from a similar elevation to that of SFLS1, however this was accompanied by very little change elsewhere on the slope.

A second smaller failure occurred in the final survey period (Figure 12C), above the SFLS1 source area. This change was accompanied by a number of other changes across the slope, also visible in Figure 12, suggesting that these were all perhaps triggered by one intense rainfall event. The large remobilisation within the SFLS1 source area was detected almost a year after initial failure. Further changes include small losses from the SDLS1 headscarp and along the margins of the first small landslide detected in July 2015.

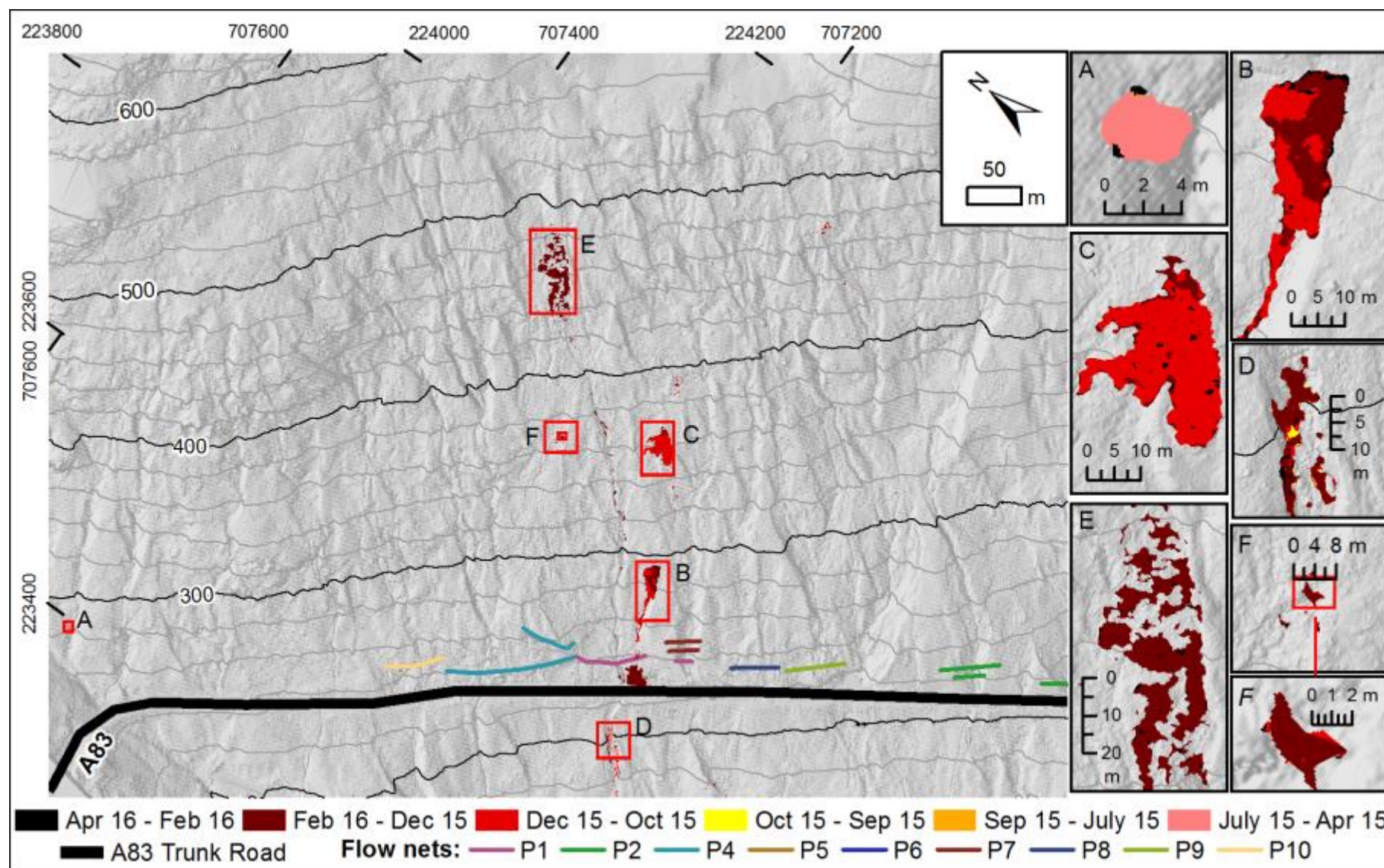


Figure 11. A composite of masked (year 1) intra-annual losses.

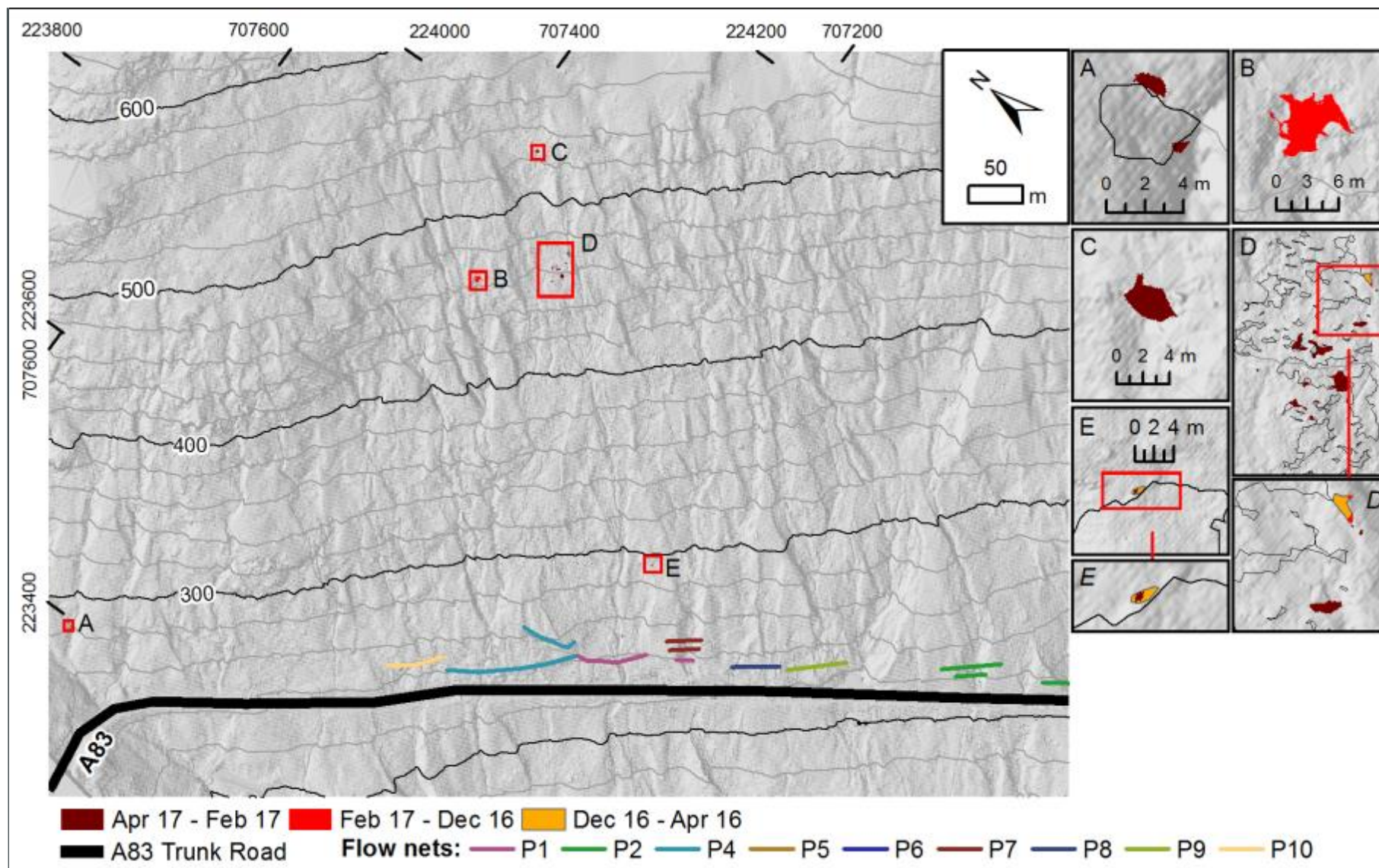
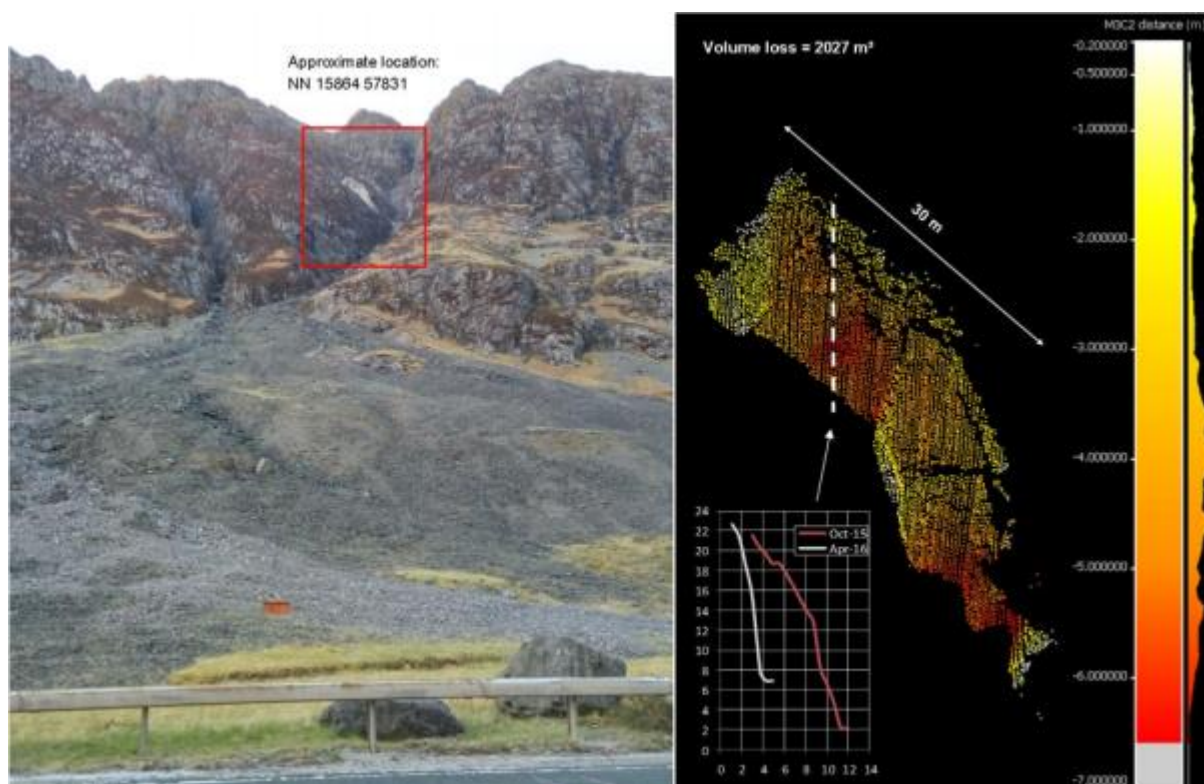


Figure 12. A composite of masked (year 2) intra-annual losses.

### 3.2.3 Other sites

Additional monitoring sites included the slopes above the A85 at Glen Ogle and the A82 at Glen Coe. Whilst some minor changes were detected ( $< 10$ ) at Glen Ogle during the monitoring period, these were isolated to the first monitoring year. It is considered that small magnitudes of change may be occurring below the site-specific detection threshold (LoD) of 0.183 m. This LoD arises from instrument precision and registration error, similar to those discussed for RabT. It is possible that small changes may be accumulating to a magnitude above this LoD, to a point where they may be detectable over longer monitoring periods. These would most likely be isolated within the main gullies, where exposed and fragmented bedrock has been observed during on-slope examinations. Two years of monitoring may have therefore not been sufficient for them to surmount the detection threshold. A continued but less-frequent monitoring schedule is therefore advised for this site, to characterise ongoing long-term activity should it be occurring.

A limited number of changes were also detected at Glen Coe, particularly above two car park scan positions (NGR NN 17090 56874 and NN 16825 56926). A large rockfall exceeding 2,000 m<sup>3</sup> (Figure 13) was however detected from a third scan position (at Achtriochtan Farm at NGR NN 15693 57149), reporting of which prompted a more detailed investigation. A lack of outflow from the gully into which it has fallen suggests the event did not pose an immediate hazard, however the failure may represent a longer-term gully recharging event, should the material degrade and discharge out of the gully at a later date, perhaps a constituent of another event.



**Figure 13. A large (> 2,000 m<sup>3</sup>) rockfall detected above Achtriochtan farm between October 2015 and April 2016.**

Small numbers of failures are known to have occurred at both the A82 Glen Coe and the A85 Glen Ogle sites since 2004. However, the nature of the Glen Coe site and the associated risks mean that continued inter-annual surveys perhaps could be justified. This would be particularly useful due to the more complex and stochastic nature of rockfalls when compared to debris flows, where initial sources and potential entrainable masses can be assessed.

### 3.3 Discussion

Monitoring has proven useful over both inter-annual and intra-annual change detection regimes, allowing detection of both small and large changes, as well as smaller changes superimposed within the domain of later larger changes. TLS data enables objective identification of new changes, where it would be difficult to differentiate between new small events and the numerous relict scars. Detection of two very small changes (Figure 12 B and C; also visible earlier in Figure 9 and Figure 8 respectively), high up on the slope in the second year of monitoring, demonstrates the capability of TLS in detecting small changes, despite the large scan distances. Many of these smaller changes are difficult to identify by eye or with photographs alone. Small detected failures cannot be isolated to a precise date using TLS alone, however intra-annual data affords a smaller time range within which precise event timings can be identified using supplementary data such as high-frequency photographs. This form of scrutiny is important to other forms of analysis including that of rainfall data for the purpose of developing and understanding intensity-duration thresholds.

Although TLS data was not required to detect the notable SDLS1 event, the technique did detect incision of a new truncated gully below the source area. Identification of this erosion would have been particularly difficult, as incision and deposition both result in exposed sediments with similar appearances. Debris flow runout paths (2007 and 2009) are known to have previously connected at RabT, leading to rapid development of a major gully. The SFLS1 event also appears to have coupled with this channel, after which further sediment loss has occurred within the SFLS1 source area, perhaps representing continued incision and channel establishment. Rapid incision of a new truncated gully by the SDLS1 debris flow appears to support the hypothesis that debris flows are a more significant agent of gully development than previously thought. Evidence of further channel development, through continued monitoring, is however desired to further develop this hypothesis.

TLS data also was not required to identify the SDLS2 event, however such data enabled quantification of the event magnitude, in particular the distribution of sediment following failure. Prior to this project, this significance of small events in loading gullies for future entrainment was perhaps unclear albeit that Nettleton et al. (2005) and Winter et al. (2005) make reference to the episodic nature of such events and the formation and subsequent failure of debris dams.

Intra-annual change detection has enabled delineation between two mobilisations at the source area of SDLS1, where inter-annual change detected only one event (superimposed changes). The phase 1 catch net, which inhibited the first mobilisation, was emptied following the initial SDLS1 failure. It is possible that the intense rainfall which subsequently triggered SFLS1 may have also triggered remobilisation in the SDLS1 source area. Rather than a continuous stream of small failures, a single secondary failure is plausible. This seems

more likely as a further 12.5 m<sup>3</sup> loss was scoured from within the truncated channel at this time (between December 2015 and February 2016). Should this have been the case, the phase 1 catch net would have been filled by the larger SFLS1 failure and an additional 224 m<sup>3</sup> from the SDLS1 source area. Combined, these may have exceeded the catch net capacity and ultimately led to deposition on the road.

The intra-annual results at RabT have also demonstrated the propensity for landslides to repeatedly discharge sediment long after initial failure. Such observations have also been made at Wet Swine Gill in the English Lake District by Johnson & Warburton (2015) and may be of major significance to mitigation planning. Due to seasonal vegetation fluxes, intra-annual findings would not have been possible without development of a bespoke change detection approach.

Detection of a large rockfall at Glen Coe prompted investigation by road management authorities. This event may have eventually been identified without use of TLS, however monitoring prompted a more rapid response to an event with the potential to pose a major hazard. Given the stochastic nature of rockfalls at Glencoe, a high frequency of monitoring is not considered necessary. Along with the lengthy processing of data to achieve intra-annual results, high frequency intra-annual monitoring at sites such as Glen Coe and Glen Ogle may be considered overly laborious for application beyond an experimental research project. ArcMap for example is very particular about the data formats required for raster subtraction, with each dataset extent having to match perfectly and as this is rarely the case manual editing is almost always necessary.

Processing could be semi-automated using ArcMap's Model Builder, however the preceding activities of data collection, manual processing and basic change detection command approximately three days of work per survey period (more than 40 days for RabT alone throughout this two-year project). Whilst masking was found to work well, the approach also occasionally left small residual changes which required manual verification, adding to the workload required for such an approach. Inter-annual change detection has required a relatively limited amount of data processing and cleansing compared to intra-annual data, principally due to the reduced impact of seasonal vegetation under this regime (if each annual survey is conducted at roughly the same time of year). This approach should be favoured for sites such as Glen Ogle and Glen Coe.

Data in this study have been supplemented with high resolution photographs collected with an SLR camera at an effective focal length of 300 mm. The resultant panoramas were useful for validation of detected change and articulation of the precise type of change, as well as a reference when navigating around the 3D data. Furthermore, high-resolution photographs have provided evidence of ephemeral flow, previously only observed during slope-walkovers. Winter et al. (2017) summarise and appraise high resolution panoramic image production. Further work is ongoing to produce time-series ultra-high resolution imagery at approximate pixel densities of between 1,000 and 20,000/m<sup>2</sup>, depending upon the distance to the hillside. PTGui Pro has been found to be optimal for generating these much larger and more precisely calibrated panoramas.

## 4 Modelling

Models can be used predictively or to help better understand difficult to observe phenomena. Debris flow gully deposition at RabT has not been well constrained for instance, owing to the limitations of TLS based monitoring. The available monitoring data and analysis of event mass balances suggest that deposition may be significant, but this is difficult to confirm. A well calibrated debris flow model may substantiate this supposition, providing a multi-faceted basis to the hypothesis and supporting an argument for further investigation.

Similarly, small transiently-flowing drainage channels have been observed on the RabT slope and these appear to be widespread. Such channels could be responsible for some shallow failure initiations, but such activity is also difficult to observe. In this case, high resolution topographic data can be used to simulate active flow regions on the slope, to which an inventory of past failures and monitoring data can be compared.

The models discussed have many further applications, including probabilistic applications such as the simulation of potential propagation vectors and the impacts of debris flows. Here the ability for models to shed light on a wide range of slope processes, as well as their potential to simulate and assess hazards under different scenarios is demonstrated.

### 4.1 Methodology

#### 4.1.1 Runout Modelling

Numerical runout models simulate debris flow propagation and can be used in a number of ways, from mitigation design and engineering considerations to the forecasting of potential runout zones and hazard mapping. Several algorithms have been developed to model debris flows, these include FLO-2D (O'Brien et al. 1993) and the more recent DAN3D (McDougall & Hungr 2004). The runout model discussed here is called RAMMS-DF (RApid Mass Movement Simulation; Debris flow), a 2D depth-averaged lagrangian model developed by the Institute for Snow and Avalanche Research (SLF). Such models are a major improvement on prior empirical models, which have limited scope to be applied to other sites or even regions of the same slope owing to major topographical, material and magnitude variability. Whilst attempts have been made to account for topography in empirical models, these cannot be used to estimate mean flow depth or velocity, both important components of a detailed hazard assessment (Scheidl et al. 2013).

This RAMMS-DF model was chosen at the beginning of this study, due to its focus on debris flow specific parameters including impact pressures, and its continued support and development. The RAMMS model employs a straightforward, yet resourceful, GUI software environment, one which aids ease of adoption beyond a research environment. The public version of the RAMMS-DF model was updated with an entrainment module in November 2017, a feature which is not available in most other models. This compares to FLO-2D, software also used to model debris flows, which is primarily a hydrological model and does not account for such factors.

The model is presented and explained in a manual published by Bartelt et al. (2017) and is both discussed and applied in a number of published articles (i.e. Schraml et al. 2015; Vennari et al. 2016). RAMMS employs a Voellmy-fluid friction model with two main input

parameters, these being a dry-Coulomb friction coefficient  $\mu$  ( $\mu$ ) and a velocity squared drag coefficient  $\xi$  ( $\xi$ ;  $\text{m/s}^2$ ). Other customisable parameters include flow cohesion and density. Here the testing and application of the model used in this research is discussed.

#### 4.1.1.1 Sensitivity Analysis

An understanding of model sensitivity is important, particularly because fine tuning of one parameter often necessitates the compensatory adjustment of another during calibration to attain a similar runout distance. DEMs representing true topography are highly heterogeneous and a slight variation in an input parameter can result in a large difference in model output (if previously the material had stopped short of a sudden drop for example). A planar model-slope ( $32^\circ$  based upon the average slope at RabT) was thus favoured at this stage to negate the influence of surface variability. This model slope was generated by plotting a limited series of co-ordinates within Microsoft Excel (representing corners of the slope), which were imported into the software CloudCompare. Points were interpolated into 4 planes, from which 1 m resolution planar point clouds were sampled. Planes included the left and right of the slope, as well as two central planes representing a 3 m deep channel measuring 14 m across, incorporated to limit spreading.

An input hydrograph was favoured over a block failure approach, as the latter often represents an unrealistic instantaneous discharge of material. A  $100 \text{ m}^3$  failure volume was initiated at the top of the model slope, at the centre of the modelled gully. This volume was fed into the gully using an input domain measuring  $4 \times 4 \text{ m}$  and a four second hydrograph, where the max failure volume reached  $50 \text{ m}^3$  at  $t = 2 \text{ s}$  (equivalent to a maximum 3 m flow height) and moved into the gully at a velocity of 5 m/s.

Eight model runs were iteratively conducted per parameter, with a 20 % increase or decrease of the chosen parameter around a default value (visible at the top right of Figure 14) whilst all other values were locked at their default. The maximal runout distance of each model output was sampled within RAMMS and plotted in Excel. Raster datasets of deposition were also analysed in ArcMap using a 1 m grid and the Zonal statistics tool, to create plots of deposition depth over longitudinal runout distance.

#### 4.1.1.2 Back Analysis

With a greater understanding of the sensitivity of the model to individual parameters, precise TLS data were used to calibrate the model through a process called back-analysis. In this, a model is iteratively run with different parameters to produce a 'best-fit' set of parameters relative to some form of monitoring data (often photographs). In this study, high resolution TLS data have provided an accurate demarcation of several debris flows as well as their deposition magnitude and distribution.

Pixel by pixel comparison was considered as a means to assess each model output, however this was deemed too precise when considering the nuances of numerical models. Factors such as DEM scale were also considered; regardless of resolution (a relatively high 1 m in this case), DEMs represent a simplified version of true topography and may not reproduce all of the obstacles or features which act to slow or speed up a flow.



Model outputs were instead compared using 5 m longitudinal bins (ArcMap Zonal Statistics). Volumes of deposits within each bin were plotted against monitoring data sampled using the same approach. Outputs were then compared and correlated with monitoring data, with a combination of these factors considered when deciding upon the optimal set of input parameters.

The SDLS1 event had a short runout path before being inhibited by a catch net and was thus deemed unsuitable for back-analysis. Whilst data for the SDLS2 event did not have a clearly defined terminus (due to gully occlusion), the event did yield good deposition data for comparison purposes. Minimal deposition was also observed within a phase 1 catch net, providing some upper bound on the flow's mobility.

#### 4.1.1.3 Hazard Modelling

Once calibrated, RAMMS was used experimentally to model propagation potential (an element of hazard) on a discrete part of the RabT slope. One limitation of the RAMMS software is that it cannot model large extents at a high resolution (i.e.  $\sim 1$  m yielded from TLS surveys). Topographic models are therefore cropped in order to reduce computational strain and avoid crashes. A holistic assessment requires multiple iterations each with a cropped input DEM in order to achieve full slope coverage (tiled). Furthermore, these should account for propagation across DEM edges and thus an even greater number of DEMs is required for holistic coverage. The centre of the slope has exhibited significant activity within recent years, particularly during the TLS monitoring, and thus this zone was chosen for experimental application of the calibrated model.

Hazard assessments should account for the largest credible event magnitude (Parry 2016). The largest known event at RabT, measuring an initial  $473 \text{ m}^3$ , occurred in October 2014 and formed the basis of hazard modelling (i.e. initial source area magnitude). Whilst entrainment played a significant role in this event, modelling of such a factor at this stage was considered to add unnecessary complexity to what was primarily an assessment of runout potential. Furthermore, deposit distributions are not well constrained across all of the gullies, understanding of which is necessary for such application of the model.

A grid of source cells was generated across the central region of the slope, each measuring 20 m wide and 23 m long, the former equivalent to that of the October 2014 event and in fact wider than both SDLS1, SDLS2 and SFLS1. Cells were generated through use of the Fishnet tool within ArcMap. Cell lengths were slightly truncated compared to observed failures, although this was a conscious choice to reflect the longitudinally discontinuous nature of sources, often due to deposition of soil rafts at the head and other material at the toe. The 252 cells generated were split into respective polygons within ArcMap and each polygon was exported before being individually loaded into its respective model. The resultant cells each measured  $460 \text{ m}^2$ , and represented a  $473 \text{ m}^3$  source when a depth of 1.03 m (similar to the October 2014 event, although actually smaller than SDLS2) was specified.

Modelling was conducted using the best-fit parameters found in Section 4.2.1.2, namely those back-analysed using the SDLS2 event data. Five batches of 50 models were processed, each batch taking approximately six hours to process using a desktop computer with a 3.4

GHz quad-core processor (i7-4770) and 32 GB of RAM. Maximal Flow Height raster datasets were bulk exported within RAMMS. The large number of models necessitated automation of the processing of results, thus a workflow was developed to convert each raster into a representative flow vector (polyline) without the need for manual plotting.

Automation was achieved using ArcMap Modelbuilder, in which a raster iterator was used to load in all of the results with one selection. Raster datasets of the flow extents were refined using the 'fine' tool, to produce the centreline of each flow. These refined raster datasets were subsequently converted to polylines using the 'raster to polyline' tool and cleaned using the 'Trim line' tool to remove artefacts such as truncated branches. Some vectors were more sinuous than others and contained varying numbers of branches, so a simple calculation of the total line length was not considered to truly represent the flow potential. Instead, the longitudinal flow extent of each vector was calculated using bounding boxes ('minimum bounding geometry' tool within ArcMap) by which each line was symbolised on a relative scale.

#### **4.1.2 Hydrological Modelling**

Small transiently-flowing channels were observed on the slopes of RabT during and after times of intense precipitation, however such features are seldom observed, especially from a distance and when conditions are dry. Due to their proximity to source areas, it is hypothesised that such channels influence initiation of shallow failures. Whilst this could not be shown conclusively within the scope of a doctoral project, modelling of probable preferential flow lines was possible and was considered to aid interpretation of flow distribution in relation to recorded geomorphological activity.

A high resolution (0.1 m) DEM was produced from registered TLS surveys collected at RabT in April 2015. Production consisted of point data interpolation using an Inverse Weighted Distance (IDW) method (such as that employed in ArcMap), employed within the software QT Modeler. The resultant DEM was imported into ArcMap, where the 'Flow Direction' tool was used to generate a raster of slope cell orientations along which water would likely flow. Erroneous DEM sinks (artefacts; areas of accumulation that do not allow outflow) were removed from the output, before utilisation of the 'Flow Accumulation' tool. This stage resulted in a raster dataset, with each cell value representing the number of cells (upslope) that were topographically routed through that cell.

The flow accumulation raster dataset was subsequently divided into four separate raster datasets, representing accumulation counts of 5,000, 2,000, 500 and 100 (with the higher counts theoretically representing more flow). These were finally converted to polylines and visualised alongside other datasets, including a spatial inventory of events and more recent monitoring data.

---

## 4.2 Results

### 4.2.1 RAMMS Runout Modelling

#### 4.2.1.1 Sensitivity Analysis

Analysis using a model slope (Figure 14), found runout distances to be most sensitive to the cohesion parameter; a  $\pm 20\%$  variation in cohesion (around the default value of 1,000 Pa) affecting the runout distance by  $\pm 16\%$ . The model was found to also be sensitive to changes in the density parameter, however density was varied beyond the small envelope of realistic values for comparability purposes; debris flow densities typically fall within a range of  $2,000 \text{ kg/m}^3 \pm 10\%$  (i.e. Wang et al. 2017) and deposits sampled from natural flows seldom range beyond this (Iverson 1997). A density of  $2,000 \text{ kg/m}^3$  is commonly used for debris flow and is recommended by Bartelt et al. (2017). (This value has also been adopted by Transport Scotland and TRL for determining first order estimates of debris volumes from tonnages transported for disposal during post-event clean-up.) The sensitivity of model runs performed within this realistic envelope was far less significant.

Of the two principle input parameters  $\mu$  and  $\xi$ , the model was most sensitive to the latter. Low  $\xi$  values (i.e.  $100 \text{ m/s}^2$ ) resulted in a relatively flat, large depth of deposition over a short distance. Mid-range  $\xi$  values ( $300\text{--}800 \text{ m/s}^2$ ) yielded sensible runout distances, each scaling relatively linearly with iterative increases in the input parameter. These mid-range  $\xi$  values also demonstrated a marked difference to those around  $100\text{--}200 \text{ m/s}^2$  said to be typical of granular flows (Bartelt et al. 2017), in that deposition depths were less uniform with larger relief between each peak. In contrast, high  $\xi$  values (i.e.  $+80\%$  /  $900 \text{ m/s}^2$ ) resulted in more sporadic and distributed clusters of deposition further down the slope, with a lower runout distance than the  $800 \text{ m/s}^2$  input perhaps relating to model instability.

A decrease in  $\mu$  principally resulted in an increased runout distance, whilst an increase resulted in the opposite, however in both cases this was less marked than changes in other parameters.

#### 4.2.1.2 Back-analysis

Back-analysis consisted of two phases, the results from the first are shown in Figure 15. These show observation data split longitudinally (bold black line) as well as volume uncertainty deriving from a  $\sim 0.2 \text{ m}$  TLS uncertainty value. The figure further shows the LoD related uncertainty, the additional range of deposition that could exist on the slope, but which was not detected due to a detection threshold. Many of the models do initially fall within the LoD related uncertainty range, however a number of models exceed this LoD related uncertainty bound, particularly at a distance of around  $70 \text{ m}$  downslope. These results are primarily influenced by the high default cohesion value of  $1,500 \text{ Pa}$ , but also by low  $\xi$  values ( $100\text{--}300 \text{ m/s}^2$ ). The model with a low cohesion value ( $300 \text{ Pa}$ ) resulted in too little deposition, thus indicating that the true cohesion value should perhaps fall somewhere between  $400 \text{ Pa}$  and  $1,400 \text{ Pa}$ .

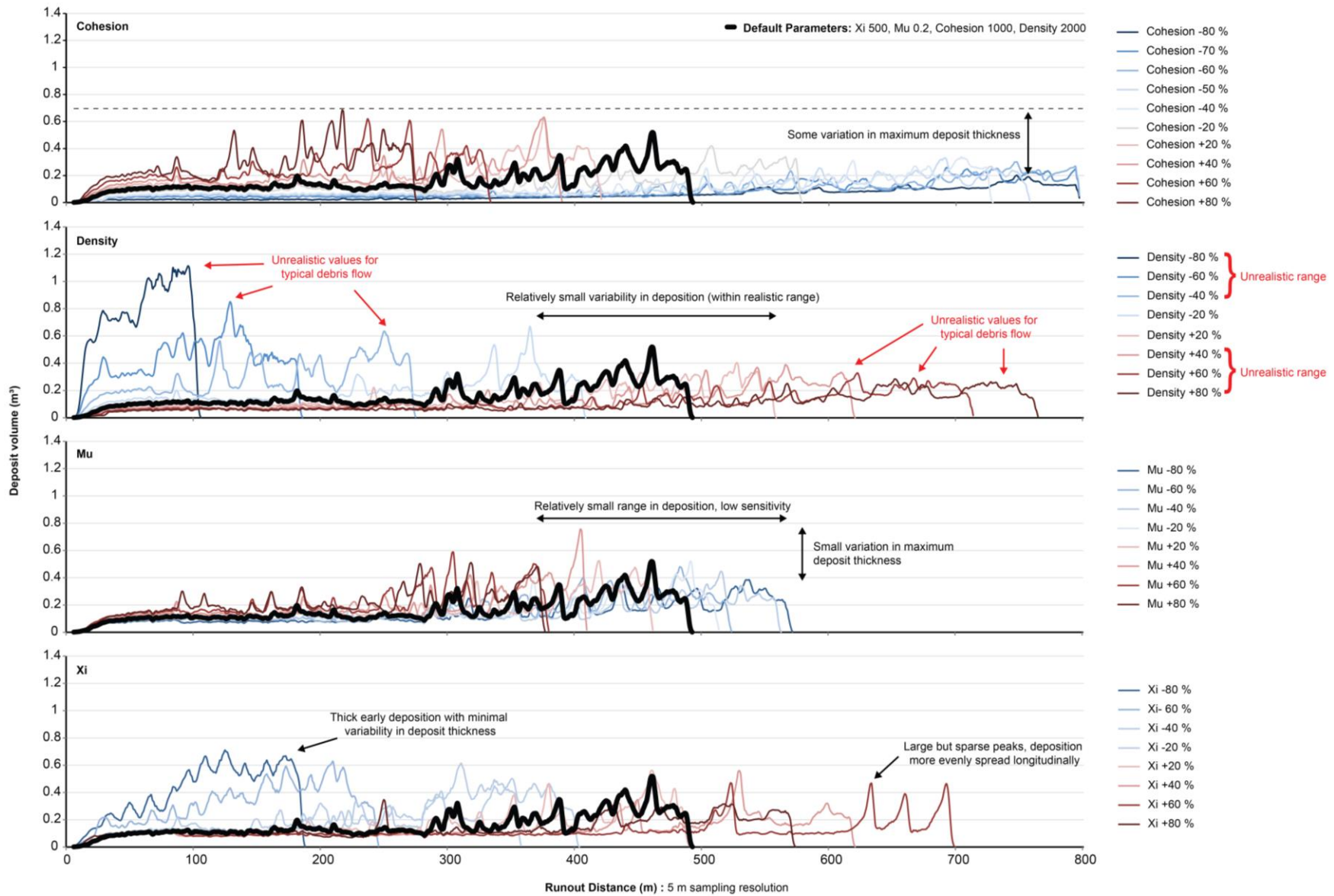


Figure 14. Sensitivity analysis of the main input parameters adopted by the RAMMS debris flow runout model.

The phase 1 plot shows that the model results do not correlate particularly with the precise observation data. This is most evident at a distance of 35 m downslope, where a large quantity of material was deposited within a short range. In the model, the largest quantities of material are also deposited here but over a longer extent, thus giving the appearance of a less pronounced peak. This likely relates to simplification of the topography within the model and of the flowing mass itself, both down to cells measuring 1 m by 1 m. Whilst being of a relatively high resolution, this may have removed or smoothed some small obstacle or change of slope within the DEM. Alternatively, the model may not have accounted for longitudinal differences in flow composition, with this large quantity of observed deposition perhaps attributable to a more granular flow head.

Figure 16 shows a second phase of refined models, based upon the findings in phase 1. In this second phase a range of input parameters were varied, starting with mid-range  $\Xi$  values and a mid-range Cohesion value of 600 Pa. These initial models yielded closer fits to the monitoring data, with the fifth model (in the legend of Figure 16) providing one of the highest correlation values (0.62). Different combinations of parameters were varied, accounting for the findings of sensitivity analysis to keep the models within a tighter range than in phase 1. Beyond phase 2, a further 49 models were conducted, however none yielded a significant improvement over those presented within phase 2.

After analysis of the initial 80 m of propagation, all second phase model outputs were analysed within the vicinity of two downslope catch nets which had been incorporated into the input DEM. Of the 26 phase 2 models, 21 far exceeded estimates of the true volume deposited within the catch net. The five remaining models (shown in bold in Figure 16) all simulated less than the estimated quantity of catch net deposition, however this was attributed to the inability of the model to account for entrainment and flow dilution. Lower than estimated deposition within the catch net was desired for this reason and so these models were considered optimal.

Of these, the initial second phase model (Figure 17) was deemed to present the most optimal all-round results. The parameters used to achieve these results are shown below in Table 2. A higher  $\Xi$  value ( $> 200 \text{ m/s}^2$ ) suggests a more muddy (fluid) flow than granular (solid-dominated) (Bartelt et al. 2017), which fits previous observations of slurry-like flows at RabT. The model also agrees with the assertion that SDLS2 charged the gully with fresh sediments, evenly spread along the gully according to the model.

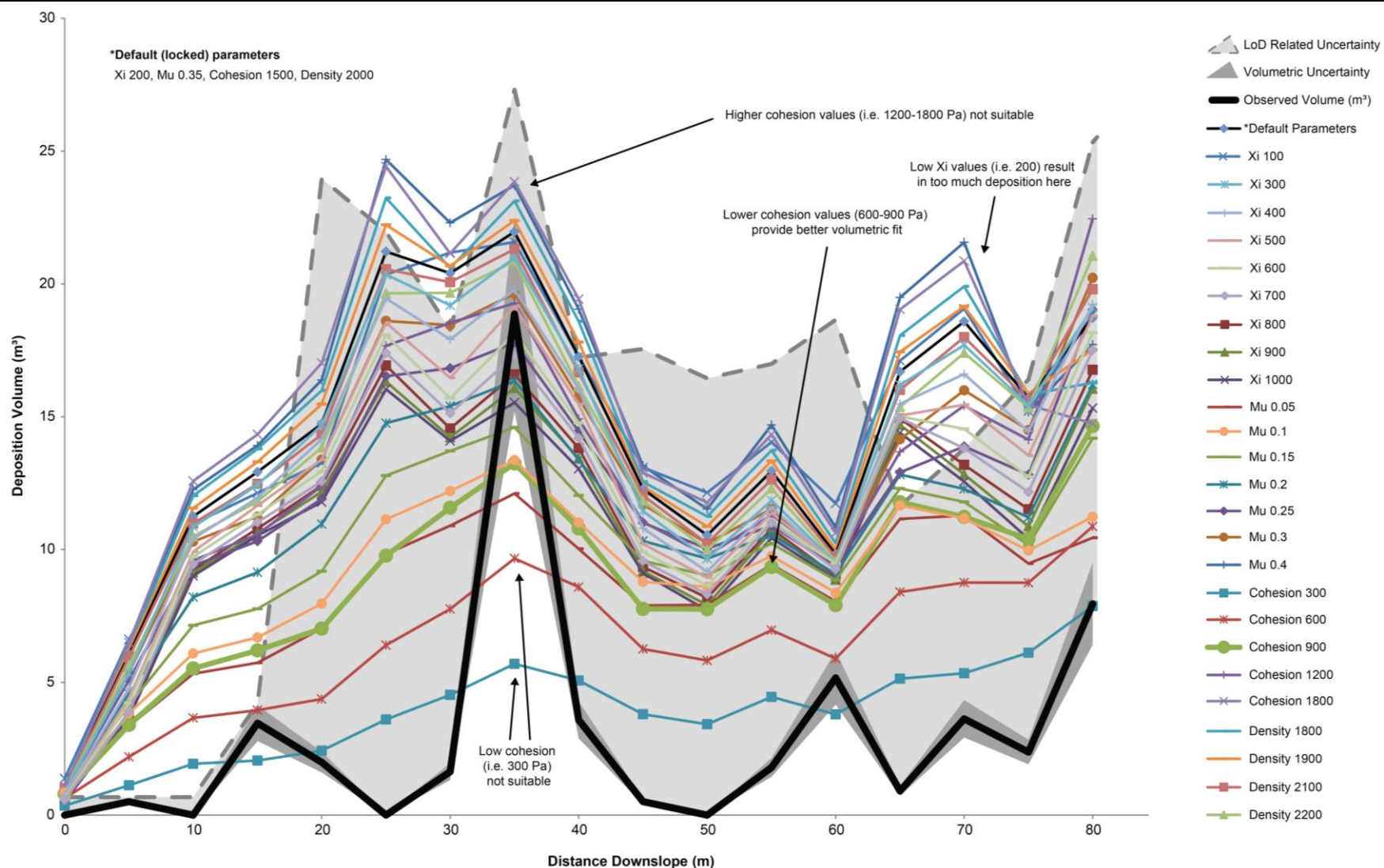


**Figure 15. Results from the first phase of back-analysis indicate that high cohesion values and low Xi values are not optimal, the first resulting in too much deposition over the 80 m extent and the latter resulting in a poor line-fit versus observation data (too much deposition, particularly to the right-hand side of the plot).**

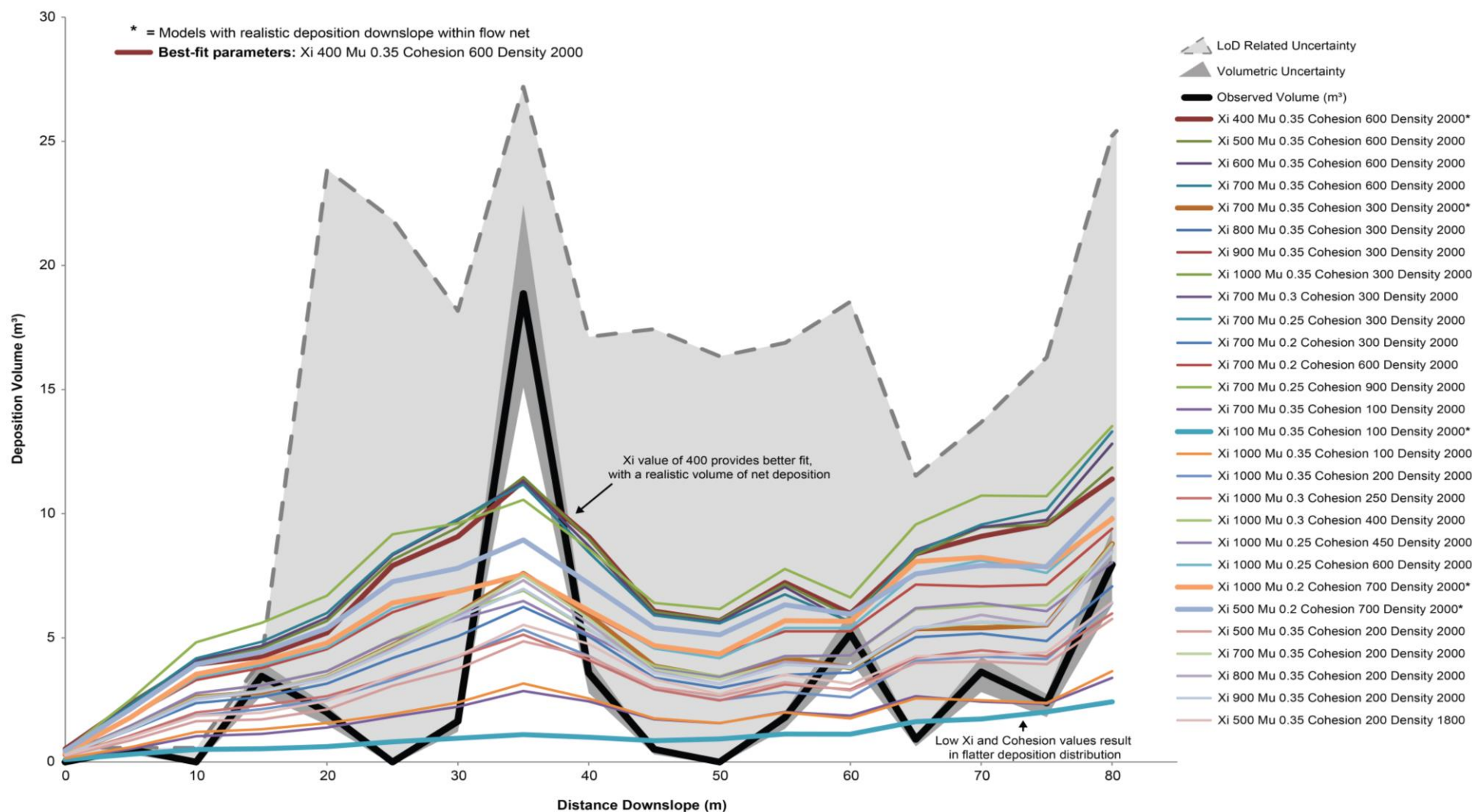
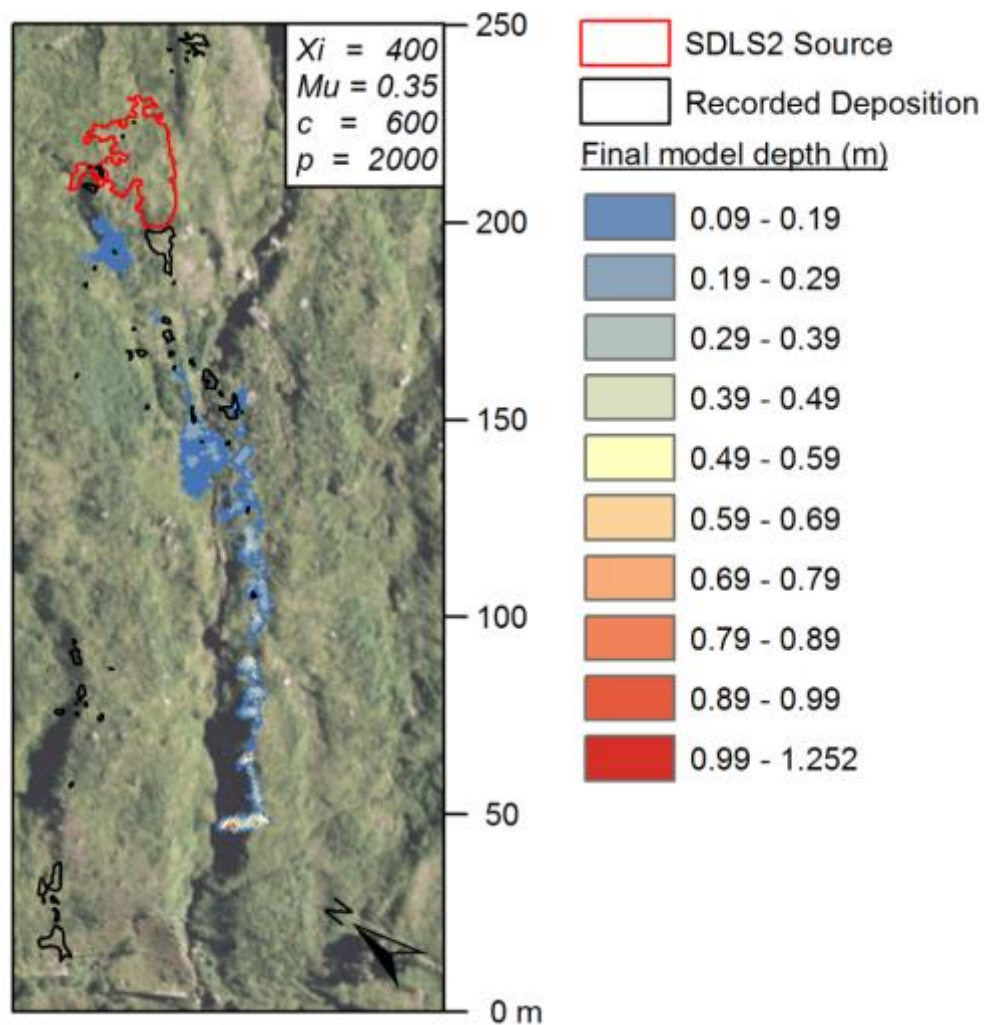


Figure 16. Results from the second phase of back-analysis indicate that a combination of mid-range Cohesion and Xi values gave a better fit with observation data. The models were conducted in the order presented in the legend to the right of the figure.



**Figure 17. The optimal model output produced during back-analysis. Deposition at a longitudinal distance of 175 m (scale on right hand side) fits observation data for the most part. Downslope (50-100 m), modelled deposition supports the assumption that the SDLS2 event lined the gully with fresh deposits down to the extent of the phase 1 catch nets. Note that the back-drop imagery is slightly offset from the DEM and model, although this does not affect the results.**



**Table 2. Optimal RAMMS input parameters for SDLS1**

<u>Parameter</u>	<u>Optimal value</u>
<b>Mu</b>	0.35
<b>Xi</b>	400 m/s <sup>2</sup>
<b>Cohesion</b>	600 Pa
<b>Density</b>	2000 kg/m <sup>3</sup>

#### 4.2.1.3 Hazard analysis

The results of the hazard analysis are shown in Figure 18. Here a series of vectors (polylines) can be seen, each representing one model originating from its respective source cell. Despite only covering the central region of the slope, the vectors clearly show zones of low and high mobility, the latter corresponding with the major gullies and demonstrating their well-known debris flow enhancing effects.

As a standalone modelling approach, the results appear to effectively highlight areas where debris flows pose a hazard as a result of high mobility. The final output from the model does not however account for additional factors such as entrainment, thus such an approach should be adopted as one step in a wider assessment. Furthermore, although the cell-based source approach offers complete coverage across the zone of interest, it does not account for failures that might occur in a zone overlapping two idealised source areas. In this application, one source may overlap two different basins, on a ridge between gullies for example. This has the effect of splitting the flow into two propagation vectors, reducing the runout potential of the flow. An idealised source 5 m to the south-east of the example may have propagated as a larger singular mass of material for example, thus representing a more mobile flow than that represented by the results. This highlights the potential need for higher resolution modelling (a greater number of idealised cells, with overlap).

Figure 19 highlights two particular cells which were found to circumvent existing catch nets, thus demonstrating the additional capability of this approach to highlight potentially unmitigated hazards. These particular models resulted in short runout distances, likely owing to the lack of confining topography. However, their source towards the bottom of the slope would at least enable partial propagation onto the road according to the model. Such vectors however represent a worst-case scenario, in which a very large quantity of material would be required to fail. These results do not therefore directly translate to a hazard. The experimental approach presented here is designed to highlight zones that may theoretically represent a hazard, allowing a more in-depth analysis of the modelled sources to assess whether such a scenario is credible: i.e. whether there is adequate material and whether the material is at all prone to failure.

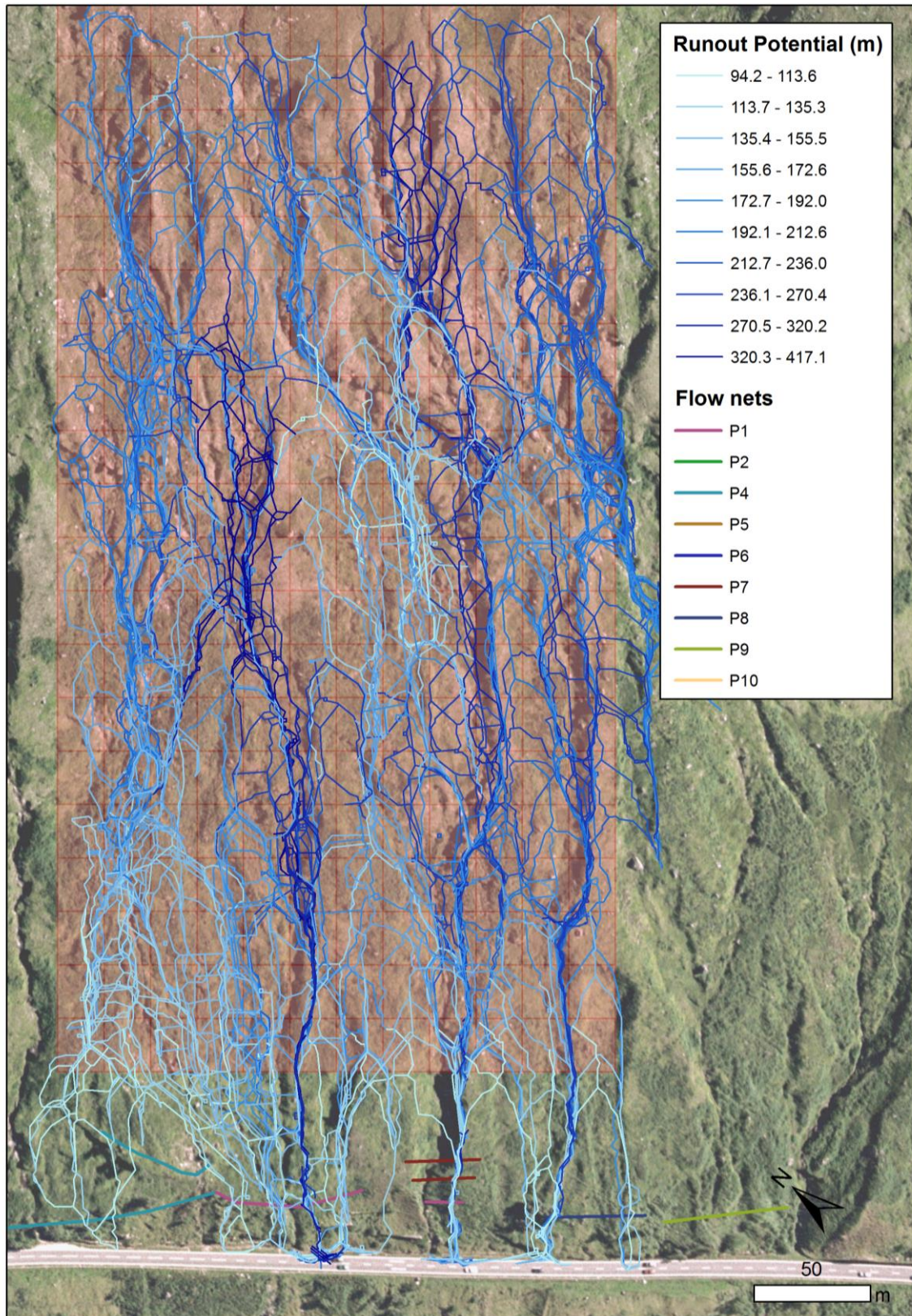


**Figure 18. Results from initial experimental hazard analysis. Red boxes represent model sources. The darkest blue lines show model vectors with the greatest longitudinal runout potential, whilst lighter blue lines highlight shorter runout potential.**

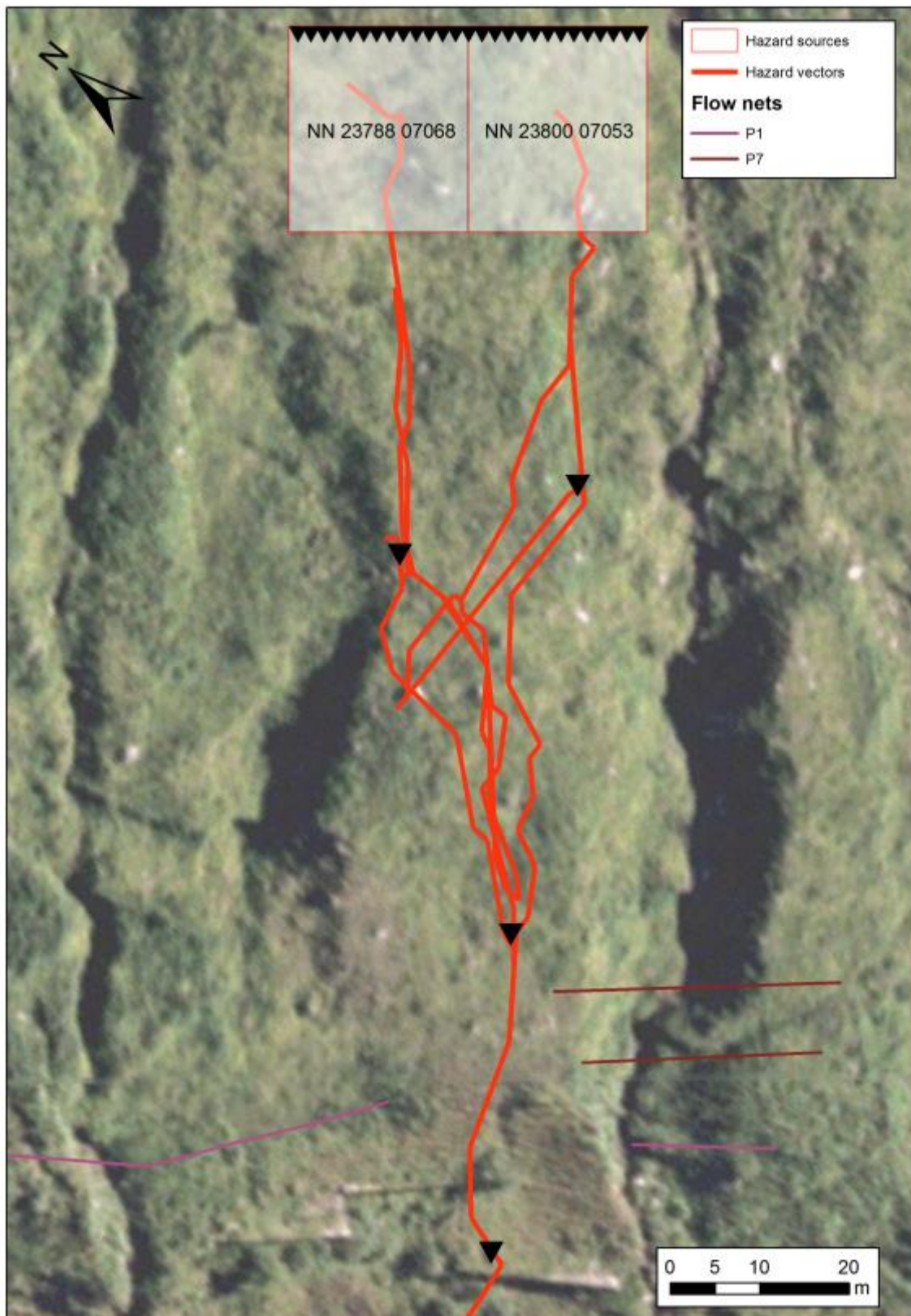
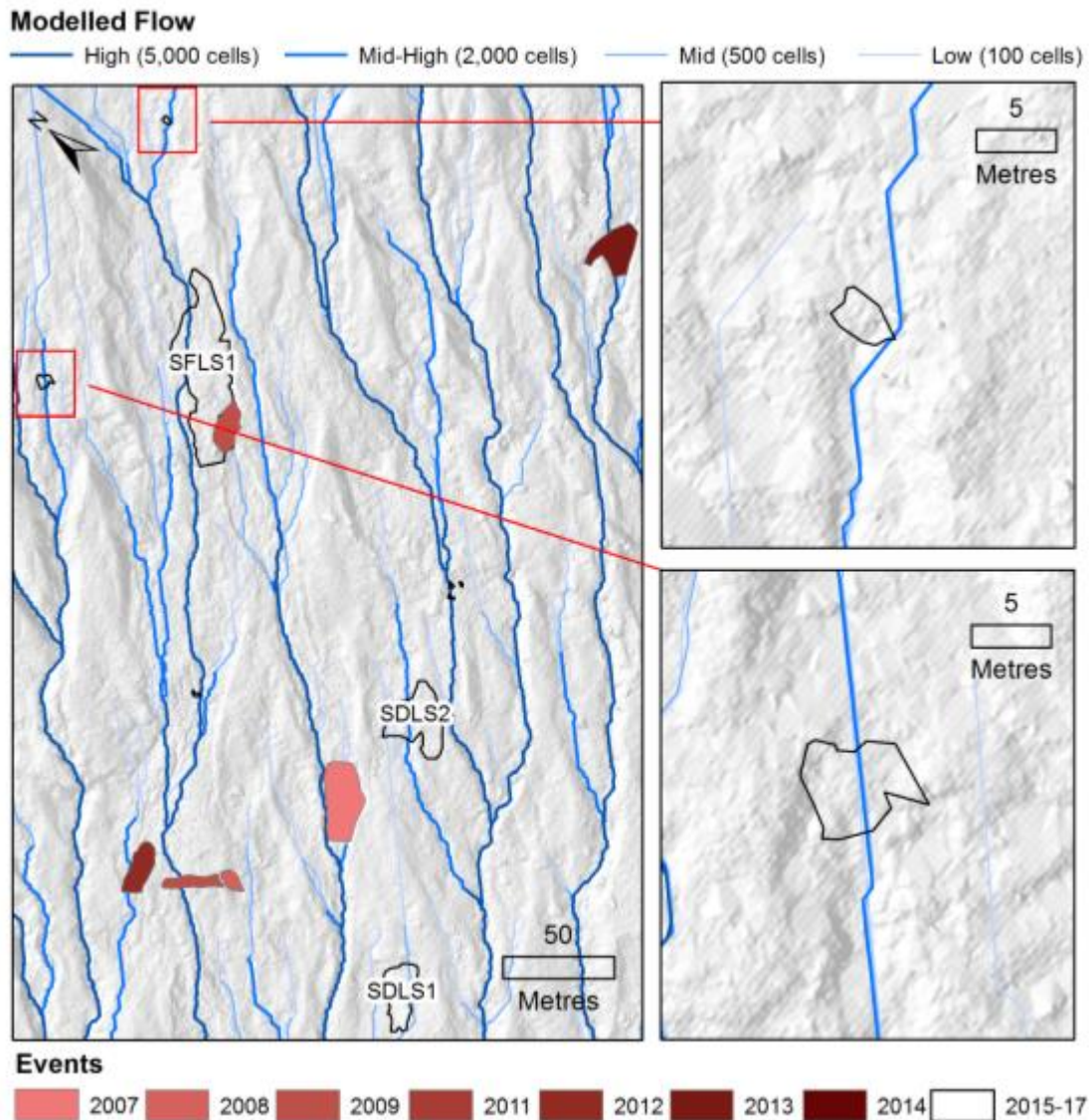


Figure 19. Two particular source cells that may represent a particular hazard to the A83 (just beyond the lower extent of the figure) due to topographic routing between catch nets. Large black triangles indicate the direction of travel along the hazard vectors. The smaller tightly spaced black triangles highlight the headscarp of the model sources.

#### 4.2.2 GIS Hydrological Modelling

Figure 20 presents an example of hydrological flow modelled within ArcMap, here presented alongside some of the change detected during the monitoring period. Drainage lines appear to coincide with the small failures detected and shown in Figure 11B and 11C, zones where flow lines are also clear within tele-photographs (Figure 8 and Figure 9). Modelling in this case has added support to the role of transient channels other than the major gullies in influencing debris flow processes and highlights the need for further research into the role of such channels in potentially triggering failures, as well as their development over time into larger more permanent features.



**Figure 20. Modelled hydrology in relation to the two small shallow failures detected during the second year of monitoring, as well as other recorded events.**

These results provide a simplified assessment of potential drainage and do not necessarily equate directly with actual slope hydrology. The analysis ignores the influence of spatially variable soil and deposit characteristics, hydrogeological conditions and features such as macro-pores. Furthermore, the model results are based upon a 0.1 m DEM and thus may not account for the effect of topographic features such as a small boulder which could entirely reroute flow along a different path. Nonetheless, the model results shown alongside small detected failures indicate and support the hypothesis that surficial drainage may influence some slope failures. Whilst not conclusive, these results highlight the need for further investigation into such a mechanism.

### 4.3 Discussion

The RAMMS debris flow model was found to be most sensitive to the cohesion parameter, this primarily affecting the runout distance of the models. This could mark the difference between a model highlighting a slope-zone as a hazard or not. Back-analysis indicated an appropriate range for this particular parameter, however modelling efforts may benefit from measurements of true cohesion in the field. Collection of such data is however a major challenge, with inter-flow variability necessitating multiple measurements. It would instead be more feasible to vary the cohesion parameter either side of the back-analysis derived value, to account for uncertainty. In application of the model, this would provide upper and lower bounds on the runout potential of each slope zone. Only one landslide event has been used for back-analysis and presented in this report. It is our intention to compare the optimal parameters from this event, with those from another back-analysed event, enabling an assessment of if and how rheologies vary between separate flow events. This will ultimately help to gauge the applicability of a model once calibrated. This additional stage may further highlight the requirement for an upper and lower bound (mobility) modelling approach. Results from this further stage of work will be presented in a final doctoral thesis in 2018 as well as a final report upon completion of the project.

The back-analysis results (SDLS2;  $\xi$  optimal parameter of 400 m/s<sup>2</sup>) suggest that debris flows at RabT are of the muddy-flow type rather than a more granular type. Whilst this was evident prior to modelling, based upon observations of slurry-like deposits on the A83 for example, the model confirms the particularly mobile nature of flows at the site and draws attention to the potential role of mixing with streamflow. A calibrated model will enable further interrogation of monitoring data, including the potential analysis of different gully entry angles and how these may impact flow momentum. Such a factor may have been influential in reducing the mobility of the SDLS2 event, ultimately resulting in mass recharge of the gully downslope.

Initial experimental hazard analysis has shown promise as a useful approach to assessing the runout potential across a large area of the slope. In the results presented, zones of greater runout potential are focused around large convergent channels or gullies, although even these respective features appear to influence runout to different degrees. It is possible that this may relate to the position of modelled source areas relative to the centre-line of the channels, with those directly in the middle perhaps resulting in more efficient flow. This may highlight the need to perform a greater number of models with overlapping source areas to negate such an effect. Furthermore, nuances and limitations of modelling mean that such

---

results should be interpreted with care. The methods presented perhaps relate more to susceptibility than to hazard and would benefit from further analysis, such as an appraisal of material availability on both the slope and within channels to truly give an indication of hazard. Nonetheless, it is considered that the approach could be applied to the rest of the slope with relative ease, for a more complete analysis. This is aided significantly by semi-automated processing of model outputs using a model developed within ArcMap Model Builder.

Hydrological modelling has demonstrated that transient flow paths potentially reactivate during times of intense rainfall, the impact of which is not yet certain but may influence slope activity. Torrential hydrological flow within well-established channels is seldom observed due to poor visibility caused by frequent intense rainfall. If small channels are activating at times of intense rainfall, it is also anticipated that major channels flow with significant volumes of water that may play a role in diluting channelised flows, thus increasing their mobility. Future investigations would benefit from monitoring of gully outflow volumes to better understand this mechanism.

## 5 Summary and Recommendations

Results from both a two-year monitoring programme and modelling using the RAMMS debris flow model have been presented in this report. Long range TLS has proven effective for monitoring slope failures at the selected sites, with multiple possible applications of the data including change detection, mapping of flow and past failure activity, interpretation (using secondary hillshade products) and numerical debris flow modelling. TLS has enabled detection of particularly small changes ( $\sim 1 \text{ m}^3$ ), demonstrating its capability to monitor a wider range of change magnitudes than was previously possible.

Detection of multiple small changes at RabT confirms the continued dynamic status of the site. Activity has included the linkage of the SFLS1 source areas with a major gully, potentially elongating the latter. Further monitoring of this slope region is required to substantiate this, however such activity has been observed in similar cases (Johnson & Warburton, 2015) and secondary mobilisations have already been detected a year after initial failure, perhaps suggesting ongoing development. The SDLS1 flow was also found to have eroded a new truncated channel in a previously consolidated area. This area of the slope should also be subject to continued monitoring, particularly as a new channel could mobilise new sediment stores. Secondary mobilisation from the SDLS1 landslide scar is of interest, as this may have occurred after the phase 1 catch fence had been emptied, refilling the structure and potentially reducing its effective capacity.

Elsewhere, detection of a large rockfall at Glen Coe, away from the road, demonstrates the stochastic and dynamic nature of geohazards at the site. This event had not been identified prior to monitoring. Reporting prompted further investigation by road management authorities and demonstrates the value of objective change detection. The large rockfall also highlights the potential for slope changes elsewhere at the site, perhaps closer to the road as a more significant hazard. Glen Ogle meanwhile, despite not demonstrating any detectable activity, may be undergoing small magnitude changes detectable over a longer timescale.

Further monitoring is recommended at RabT, and this is currently being undertaken by Transport Scotland, TRL Newcastle University and Northumbria University. Building on the findings from this study, future TLS surveys should be focused around the winter months. Annual surveys between the months of February and April should be a priority, as these months afford a good base dataset in which seasonal vegetation is at its lowest state, thus limiting the impact on subsequent loss detection. Such an approach would also minimise the otherwise lengthy data processing required. Continued monitoring would be beneficial at Glen Coe and Glen Ogle, although the hazard and risk profile at the former site may justify more frequent monitoring.

Long range TLS suffered from occlusion and attenuation in places, the latter being most problematic due to limitations of the scanning hardware. Whilst a laser scanner of increased range (Riegl LMS-VZ400; 4000 m) achieved better results, this too achieved limited coverage in gully areas where the surfaces are typically dark and wet. A longer-range laser scanner is manufactured by Riegl (VZ-6000; 6000 m range), which outputs a greater intensity laser beam and this may yet prove useful for monitoring of such areas.

---

The RAMMS debris flow model has shown significant promise in improving the understanding and potential mitigation of debris flow events, however more work is required to enable a robust appraisal of the model and its applicability to hazard analysis. Further development of the presented hazard application approach is also required, primarily to account for parameter uncertainty. The hazard modelling approach does however already show major promise in highlighting areas of the slope that may amplify the debris flow geohazard, as well as identifying areas where mitigation work should be focused. Modelling and mapping of slope hydrology will aid further analysis of slope changes, particularly those arising from continued monitoring. Additional events, particularly small shallow failures, may provide further evidence of a link between hydrology and shallow failures. Several small failures have already been identified beyond the timespan of the two-year monitoring programme presented in this report. This again demonstrates the need for continued research at sites such as RabT.



---

## 6 Conclusions

The results of this study have demonstrated the ability of Terrestrial Laser Scanning to detect small changes ( $\sim 1 \text{ m}^3$ ) at ranges in excess of 1 km. Seasonal vegetation changes have necessitated the development of an agile survey approach and processing workflow, with the former focused around the winter months after large scale dieback of bracken (*Pteridium aquilinum*). Findings at the A83 Rest and be Thankful have highlighted a range of important factors relating to geomorphological activity and hazard management. Findings include the potential relationship between small failures and transient hydrology, the latter reactivated at times of intense precipitation and potentially initiating failure. Debris flows have also been found to directly incise the slope, developing areas which could be prone to future erosion and yield shallow failures. Recent source areas have released sediment many months after failure, a factor which may be of major importance to the active management of mitigation structures, such as catch nets and culverts which have finite capacities. Small events of limited mobility have also been shown to fill gullies, potentially facilitating later flow magnitude increases and thus generating a greater hazard.

New sediment inputs could be mapped alongside existing stores, to form a site-specific hazard map accounting for potential entrainment. Such analysis would benefit from continued monitoring, which is recommended at the A83 Rest and be Thankful on a sub-annual basis. The months of March and April are considered optimal to encompass the lowest vegetation state and entire winter period. The A85 Glen Ogle and A82 Glen Coe have demonstrated a relatively small number of changes over the monitoring period. As such, it is recommended that both sites be continually surveyed on a less frequent basis (annual or less), also around the winter months.

Modelling has proven a potentially useful tool in simulating and forecasting future hazard and slope development areas, including those prone to transient (reactivated) hydrology. These could also be fed into a hazard mapping workflow, alongside TLS findings, to develop a new hazard mapping approach. Questions remain about the heterogeneity of events at the same site however and thus the appropriate method to account for such uncertainty requires further consideration. A doctoral thesis, currently under development, and subsequent final project report will expand on this investigation, as well as concluding further analysis of monitoring data presented in this report.



---

## Acknowledgements

The authors gratefully acknowledge funding from the Scottish Road Research Board, Transport Scotland and Northumbria University.



## References

- Ballantyne, C. K. 1986. Landslides and slope failures in Scotland: a review. *Scottish Geographical Magazine*, **102**(3), 134-150. doi: 10.1080/00369228618736667.
- Bartelt, P., Bieler, C., Buhler, Y., Christen, M., Deubelbeiss, Y., Graf, C., McArdell, B., Salz, M. & Schneider, M. 2017. *RAMMS debris flow user manual V1.7*. Available at: [http://ramms.slf.ch/ramms/downloads/RAMMS\\_DBF\\_Manual.pdf](http://ramms.slf.ch/ramms/downloads/RAMMS_DBF_Manual.pdf).
- Benda, L. E. & Cundy, T. W. 1990. Predicting deposition of debris flows in mountain channels, *Canadian Geotechnical Journal*, **27**(4), 409-417. doi: 10.1139/t90-057.
- Besl, P. J. & McKay, N. D. 1992. A method for registration of 3-D shapes. *IEEE Transactions on Pattern Analysis and Machine Intelligence*, **14**(2), 239-256. Available at: [http://eecs.vanderbilt.edu/courses/cs359/other\\_links/papers/1992\\_besl\\_mckay\\_ICP.pdf](http://eecs.vanderbilt.edu/courses/cs359/other_links/papers/1992_besl_mckay_ICP.pdf) (Accessed: 30 June 2017).
- Bocco, G. 1991. Gully erosion: processes and models. *Progress in Physical Geography*, **15**(4), 392-406. doi: 10.1177/030913339101500403.
- Bovis, M. J. & Jakob, M. 1999. The role of debris supply conditions in predicting debris flow activity. *Earth Surface Processes and Landforms*, **24**, 1039-1054. doi: 10.1002/(SICI)1096-9837(199910)24:11<1039::AID-ESP29>3.0.CO;2-U.
- British Geological Survey. 2007. Analytical Poster: 2007 Landslide at the Rest and be Thankful. Available at: <http://www.bgs.ac.uk/downloads/start.cfm?id=1245>.
- Corominas, J. & Moya, J. 2008. A review of assessing landslide frequency for hazard zoning purposes. *Engineering Geology*, **102**(3-4), 193-213. doi: 10.1016/j.enggeo.2008.03.018.
- Davies, T. R. H. 1982. Spreading of rock avalanche debris by mechanical fluidization. *Rock Mechanics and Rock Engineering*, **15**(1), 9-24. doi: 10.1007/BF01239474.
- Delannay, R., Valance, A., Mangeney, A., Roche, O. & Richard, P. 2017. Granular and particle-laden flows: from laboratory experiments to field observations. *Journal of Physics D: Applied Physics*, **50**(5). doi: 10.1088/1361-6463/50/5/053001.
- Dietrich, A. & Krautblatter, M. 2017. What does control debris-flow channel-bed erosion? A LiDAR-based change detection compared to velocity, momentum and pressure derived from a calibrated model. *Proceedings, 19th EGU General Assembly 2017*, **17**. EGU 2017 held 23-28 April 2017 in Vienna, Austria. Available at: <http://adsabs.harvard.edu/abs/2017EGUGA..1915155D> (Accessed: 16 October 2017).
- Fey, C. & Wichmann, V. 2017. Long-range terrestrial laser scanning for geomorphological change detection in alpine terrain - handling uncertainties. *Earth Surface Processes and Landforms*, **42**(5), 789-802. doi: 10.1002/esp.4022.
- Geobruigg 2015. Landslide in Scotland successfully stopped. Available at: <https://www.geobruigg.com/en/Landslide-in-Scotland-successfully-stopped-77941,7870.html> (Accessed: 19 December 2017).
- Innes, J. L. 1983. Lichenometric dating of debris-flow deposits in the Scottish Highlands. *Earth Surface Processes and Landforms*, **8**(6), 579-588. Available at:

<http://onlinelibrary.wiley.com/doi/10.1002/esp.3290080609/abstract> (Accessed: 23 December 2014).

Iverson, R. M. 1997. The physics of debris flows. *Reviews of Geophysics*, **35**(3), 245-296. doi: 10.1029/97RG00426.

Iverson, R. M. 2014. Debris flows: behaviour and hazard assessment. *Geology Today*, **30**(1), 15-20. doi: 10.1111/gto.12037.

Iverson, R. M., Reid, M. E., Logan, M., LaHusen, R. G., Godt, J. W. & Griswold, J. P. 2011. Positive feedback and momentum growth during debris-flow entrainment of wet bed sediment. *Nature Geoscience*, **4**(2), 116-121. doi: 10.1038/ngeo1040.

Jaboyedoff, M., Oppikofe, T., Abellán, A., Derron, M.-H., Loye, A., Metzger, R. & Pedrazzini, A. 2012. Use of LIDAR in landslide investigations: a review. *Natural Hazards*, **61**(1), 5-28. doi: <https://doi.org/10.1007/s11069-010-9634-2>.

Johnson, R. M. & Warburton, J. 2015. Sediment erosion dynamics of a gullied debris slide: a medium-term record. *CATENA*, **127**, 152-169. doi: 10.1016/j.catena.2014.12.018.

Kean, J. W., McCoy, S. W., Tucker, G. E., Staley, D. M. & Coe, J. A. 2013. Runoff-generated debris flows: observations and modeling of surge initiation, magnitude, and frequency. *Journal of Geophysical Research: Earth Surface*, **118**(4), 2190-2207. doi: 10.1002/jgrf.20148.

Lague, D., Brodu, N. & Leroux, J. 2013. Accurate 3D comparison of complex topography with terrestrial laser scanner: application to the Rangitikei canyon (N-Z). *ISPRS Journal of Photogrammetry and Remote Sensing*, **82**, 10-26. doi: 10.1016/j.isprsjprs.2013.04.009.

Lim, M., Petley, D. N., Rosser, N. J., Allison, R. J., Long, A. J. & Pybus, D. 2005. Combined digital photogrammetry and time-of-flight laser scanning for monitoring cliff evolution. *The Photogrammetric Record*, **20**(110), 109-129. doi: 10.1111/j.1477-9730.2005.00315.x.

McDougall, S. & Hungr, O. 2004. A model for the analysis of rapid landslide motion across three-dimensional terrain. *Canadian Geotechnical Journal*, **41**(6), 1084-1097. doi: 10.1139/t04-052.

Met Office. 2016. UK climate averages 1981-2010. Available at: <http://www.metoffice.gov.uk/public/weather/climate/> (Accessed: 28 September 2016).

Milne, F. D., Werritty, A., Davies, M. C. R. & Brown, M. J. 2009. A recent debris flow event and implications for hazard management. *Quarterly Journal of Engineering Geology and Hydrogeology*, **42**(1), 51-60. doi: 10.1144/1470-9236/07-073.

Milne, F. D., Brown, M. J. & Werritty, A. 2010. A hazardous channelized debris flow in Glen Ogle, Stirlingshire. *Scottish Journal of Geology*, **46**(2), 181-189. doi: 10.1144/0036-9276/01-409.

Nettleton, I. M., Tonks, D., M Low, B., MacNaughton, S. & Winter, M. G. 2005. Debris flows from the perspective of the Scottish Highlands. *Landslides and Avalanches: ICFL 2005 Norway* (Eds: Senneset, K., Flaate, K. & Larsen, J. O.), 271-277. Taylor & Francis, London.

Neugirg, F., Kaiser, A., Huber, A., Heckmann, T., Schindewolf, M., Schmidt, J., Becht, M. & Haas, F. 2016. Using terrestrial LiDAR data to analyse morphodynamics on steep

unvegetated slopes driven by different geomorphic processes. *CATENA*, **142**, 269-280. doi: 10.1016/j.catena.2016.03.021.

O'Brien, J. S., Julien, P. Y. & Fullerton, W. T. 1993. Two-dimensional water flood and mudflow simulation. *Journal of Hydraulic Engineering*, **119**(2), 244-261. doi: 10.1061/(ASCE)0733-9429(1993)119:2(244).

Parry, S. 2016. Landslide hazard assessments: problems and limitations: examples from Hong Kong. In: *Developments in Engineering Geology* (Eds: Eggers, M J, Griffiths, J S, Parry, S & Culshaw, M G). Engineering Geology Special Publications **27**, 135-145. Geological Society, London. doi: 10.1144/EGSP27.12.

Petrascheck, A. & Kienholz, H. 2003. Hazard assessment and mapping of mountain risks in Switzerland. *Proceedings, International Conference on Debris-Flow Hazards Mitigation: Mechanics, Prediction, and Assessment* (Eds: Rickenmann, D. & Chen, C.L.), 25-38. Available at: <http://www.scopus.com/inward/record.url?eid=2-s2.0-3142698759&partnerID=40&md5=9a8ced2ea5a96fbf26db3fcd5f06492d>.

Rickenmann, D. 2005. Runout prediction methods. *Debris-flow Hazards and Related Phenomena* (Eds: Jakob, M. & Hungr, O.), 305-321. Springer, Heidelberg.

Rosser, N., Lim, M., Petley, D., Dunning, S. & Allison, R. 2007. Patterns of precursory rockfall prior to slope failure. *Journal of Geophysical Research*, **112**(F4), p.F04014. doi: 10.1029/2006JF000642.

Scheidl, C., Rickenmann, D. & McArdell, B. W. 2013. Runout prediction of debris flows and similar mass movements. In: *Landslide Science and Practice Environments: Volume 5, Complex Environment* (Eds: Margottini, C., Canuti, P. & Sassa, K.), 221-229. Springer, Heidelberg. doi: 10.1007/978-3-642-31310-3\_30.

Schraml, K., Thomschitz, B., McArdell, B. W., Graf, C. & Kaitna, R. 2015. Modeling debris-flow runout patterns on two alpine fans with different dynamic simulation models, *Natural Hazards and Earth System Science*, **15**(7), pp. 1483-1492. doi: 10.5194/nhess-15-1483-2015.

Schurch, P., Densmore, A. L., Rosser, N. J. & McArdell, B. W. 2011. Dynamic controls on erosion and deposition on debris-flow fans. *Geology*, **39**(9), 827-830. doi: 10.1130/G32103.1.

Sparkes, B., Dunning, S., Lim, M. & Winter, M. G. 2017. Characterisation of recent debris flow activity at the Rest and Be Thankful, Scotland. In: *Advancing Culture of Living with Landslides: Volume 5, Landslides in Different Environments* (Eds: Mikoš, M, Vilímek, V, Yin, Y & Sassa, K), 51-58. Springer, Heidelberg. doi: 10.1007/978-3-319-53483-1\_8.

Strachan, G. J. 2015. Debris flow activity and gully propagation: Glen Docherty, Wester Ross. *Scottish Journal of Geology*, **51**(1), 69-80. doi: 10.1144/sjg2014-013.

Takahashi, T. 2014. *Debris flow: mechanics, prediction and countermeasures*: 2<sup>nd</sup> Edition, 541p. CRC Press, London.

Available at:

<https://books.google.co.uk/books?hl=en&lr=&id=jSzMBQAAQBAJ&oi=fnd&pg=PP1&dq=takahashi+2014&ots=FgxxDekdhi&sig=TaWHgk8iEft6zOPdc7UeFlfjJmQ> (Accessed: 7 October 2016).

- 
- Vennari, C., McArdell, B., Parise, M., Santangelo, N. & Santo, A. 2016. Implementation of the RAMMS DEBRIS FLOW to Italian case studies. *Proceedings, 18<sup>th</sup> EGU General Assembly 2016*, **18**. EGU 2016 held 17-22 April, 2016 in Vienna, Austria.
- Wang, B., Li, Y., Liu, D. & Liu, J. 2017. Debris flow density determined by grain composition. *Landslides*, 1-9. (Online First.) doi: 10.1007/s10346-017-0912-x.
- Winter, M. G. 2014. A strategic approach to landslide risk reduction. *International Journal of Landslide and Environment*, **2**(1), 14-23.
- Winter, M. G. & Shearer, B. 2014. Climate change and landslide hazard and risk in Scotland. In: *Engineering Geology for Society and Territory - Volume 1: Climate Change and Engineering Geology* (Eds: Lollino, G, Manconio, A, Clague, J, Shan, W & Chiarle, M). 411-414. Springer, Heidelberg. doi: 10.1007/978-3-319-09300-0\_78.
- Winter, M. G., Macgregor, F. & Shackman, L. (Eds.) 2005. *Scottish road network landslides study*, 119p. Trunk Roads: Network Management Division Published Report Series. The Scottish Executive, Edinburgh.
- Winter, M. G., Heald, A., Parsons, J., Shackman, L. & Macgregor, F. 2006. Scottish debris flow events of August 2004. *Quarterly Journal of Engineering Geology and Hydrogeology*, **39**(1), 73-78.
- Winter, M. G., Macgregor, F. & Shackman, L. (Eds.). 2009. *Scottish road network landslides study: implementation*, 278p. Transport Scotland Published Report Series. Transport Scotland, Edinburgh.
- Winter, M. G., Dent, J., Macgregor, F., Dempsey, P., Motion, A. & Shackman, L. 2010. Debris flow, rainfall and climate change in Scotland. *Quarterly Journal of Engineering Geology and Hydrogeology*, **43**(4), 429-446. doi: 10.1144/1470-9236/08-108.
- Winter, M. G., Sparkes, B., Dunning, S. A. & Lim, M. 2017. Landslides triggered by Storm Desmond at the A83 Rest and be Thankful Scotland: panoramic photography as a potential monitoring tool. *Published Project Report PPR824*. TRL Limited, Wokingham.





Landslides can cause potentially costly damage and disruption to Scottish road infrastructure. Debris-flows, a fast-moving torrent of solids mixed with water, are by far the most frequent cause and are capable of wide-reaching impacts, due to their high mobility. Many debris flow events have been recorded across Scotland, particularly at the highly active Rest and be Thankful (RabT). This report builds on previous work on debris flows in Scotland. It demonstrates the potential of Terrestrial Laser Scanning and modelling to enable a better understanding of the hazards, particularly runout. A key finding of the monitoring has been the segregation of slope failure processes into either the modification of existing hillslope gully systems (producing net deposition or scour), or the development of new channels or channel regions. Both effects are significant, as they may result in the release of otherwise consolidated/poorly consolidated sediment stores.

## Other titles from this subject area

- PPR 824** Landslides triggered by Storm Desmond at the A83 Rest and be Thankful, Scotland: panoramic photography as a potential monitoring tool. Type report details here. M G Winter, B Sparkes, S A Dunning & M Lim. 2017
- PPR 800** Assessing the risks to infrastructure from coastal storms in a changing climate. F D Milne, M G Winter, S J Reeves, J K Knappett, S Dawson, A Dawson, D Peeling, J Peeling & M J Brown. 2016
- PPR 794** Some aspects of the interaction between landslides and forestry operations. M G Winter. 2016
- PPR 650** Climate change and landslide hazard and risk - a Scottish perspective. M G Winter & B Shearer. 2013

## TRL

Crowthorne House, Nine Mile Ride,  
Wokingham, Berkshire, RG40 3GA,  
United Kingdom

T: +44 (0) 1344 773131

F: +44 (0) 1344 770356

E: [enquiries@trl.co.uk](mailto:enquiries@trl.co.uk)

W: [www.trl.co.uk](http://www.trl.co.uk)

ISSN 2514-9652

ISBN 978-1-912433-30-8

**PPR852**